A STUDY OF THE POISSON ERRORS IN THE CONVOLUTION BACKPROJECTION ALGORITHM FOR COMPUTERIZED TOMOGRAPHY

by

MAHESH VAIDYA

NUCLEAR ENGINEERING AND TECHNOLOGY PROGRAMME

INDIAN INSTITUTE OF TECHNOLOGY KANPUR

MAY, 1991

A STUDY OF THE POISSON ERRORS IN THE CONVOLUTION BACKPROJECTION ALGORITHM FOR COMPUTERIZED TOMOGRAPHY

A Thesis Submitted

In Partial Fulfillment of the Requirements

for the Degree of

MASTER OF TECHNOLOGY

by

MAHESH VAIDYA

to the

NUCLEAR ENGINEERING AND TECHNOLOGY PROGRAMME

INDIAN INSTITUTE OF TECHNOLOGY

KANPUR

MAY, 1991

NETP- 1991 - M - VAI - STU

D E D I C A T E D

T O M Y

P A R E N T S

CERTIFICATE

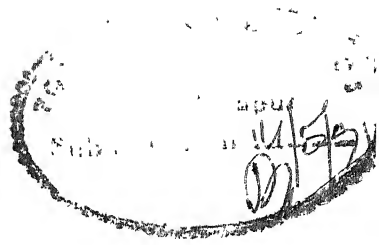

This is to certify that this work on "A STUDY OF THE POISSON ERRORS IN THE CONVOLUTION BACKPROJECTION ALGORITHM FOR COMPUTERIZED TOMOGRAPHY" by Mr Mahesh Vaidya has been carried out under my supervision and has not been submitted elsewhere for the award of a degree.

May 1991

[PRABHAT MUNSHI]

Assistant Professor
Nuclear Engineering and Technology Programme
I.I.T Kanpur

ABSTRACT

The technique of reconstruction tomography used widely in diagnostic radiology has been successfully adapted to measure density in bubbly air-water flows. The 'convolution back-projection' algorithm, in conjunction with the Ramachandran-Lakshminaraynan filter has been used for reconstruction in the form of a density distribution of a cross- section. The process of data acquisition is governed by photon statistics, which follow the laws of Poisson random variables.

In this study, a Poisson error has been imposed on the projection data and the consequent effects on the reconstructed profiles has been studied. It has been observed that the process of reconstruction is more vulnerable to uncertainities in the region very close to the centre of the pipe. Also, the need for a gamma-ray source stronger than 13 mCi is reflected in the results.

ACKNOWLEDGEMENTS

I wish to express my indebtedness to Dr. Prabhat Munshi for his invaluable guidance, his accessibility and unlimited co-operation during the course of study. It was only due to his moral support that an uninitiate like me could attempt a project in this fascinating field. It was a nice experience to work under him.

I am grateful to my family for consistently encouraging me despite the distance.

I cannot forget the tasty meals I had, thanks to Mrs. Munshi. It certainly alleviated the monotony of the hostel food.

I sincerely acknowledge the support of the entire NET family.

My sincere thanks to my friends and colleagues for the helpful discussions, inspiration and co-operation throughout my stay over here.

A special thanks to the ubiquitous Yankee Doodle virus, without which my sense of fulfillment would have been incomplete.

TABLE OF CONTENTS

LIST OF FIGURES

LIST OF TABLES

NOMENCLATURE

A	Cut-off frequency in the spatial frequency domain
c	Path of radiation
CAT	Computer Aided Tomography
CBP	Convolution backprojection
F	Spatial frequency
FBG	Fan beam geometry
NRAY	Number of rays in a view
NVIEW	Number of views
$p(s;\theta)$	Projected data
PBG	Parallel beam geometry
W(F)	Window or filter function
α	Void-fraction of the two-phase flow at a point
$\langle\alpha\rangle$	Cross-sectional averaged α
$\mu(r,\phi)$	Point dependent attenuation coefficient of the material
Δs	Distance between two consecutive parallel lines
ρ	Density of the given material
θ	Angle between the Y-axis and the given ray in PBG

CHAPTER 1

INTRODUCTION

Computerized tomography, which revolutionized the area of medical imaging, is being increasingly used in a variety of non-medical areas such as nondestructive testing (NDT) and two-phase flow measurement. One of the major problems confronting a nuclear engineer is the measurement of void fraction during a "loss of coolant accident" (LOCA). Tomographic techniques are very useful in such instances due to their accuracy and reliability.

In many applications, in which measurement of cross-sectional distribution of any property is required, we can make only indirect measurements by probing the object with invisible, penetrating radiation, and then interpret these measurements. Often, this measured data is not directly interpretable, but is related to the cross-sectional distribution (of the relevant property) in a known way. The general aim of all image reconstruction procedures is to process the data to form a cross-sectional image, thus facilitating the interpretation of the measurements. To determine the density of the object under test, various strip integrals (of a parameter like the attenuation coefficient) corresponding to a particular angle of view are taken. This set of strip integrals is called a projection of the object. Given a number of such projections at different angles of view, the estimation of the corresponding distribution (of attenuation coefficient or another parameter) within the object is the basic problem of image reconstruction from projections

Computerized Axial Tomography (CAT) is the most significant application to date, of this technique.

The mathematical principles, which form the basis of this technique, are attributed to Radon [1], who showed that any arbitrary function can be reconstructed provided all of its line integrals are known. However, the method of Radon could not be implemented due to the inherent mathematical complexities. Bracewell reported an application of CT in radio astronomy [2] and Cormack [3] derived an inversion formula which was closer to being implementable compared to Radon's solution. Bracewell and Riddle [2] and Ramachandran and Lakshminarayan [4] showed how computations involved in the CT methodology could be accelerated by adopting the use of convolutions. However, it was almost 50 years after the publication of Radon's paper that a CT machine was pioneered by Hounsfield [5], in the year 1970.

The applications of tomography can be found in such diverse and wide ranging areas like radio-astronomy [2] and electron-microscopy [4]. Butchers have used CT scanners to estimate the quality of meat prior to slaughter [6]. Use of CT scanners to inspect wooden poles used in power transmission has also been reported [7].

The present study is an effort towards studying the effect of the errors in the data collection by a gamma-ray counting set-up. The physical laws of nuclear decay are such that their intrinsic statistical variations have a Poisson distribution. This implies that the projection data used in reconstructing the image has an error term inherent to it. In this study, this error term has been replicated by incorporating

pseudo-random numbers in the projection data and the consequent effects on the reconstructed profiles investigated.

CHAPTER 2

PRELIMINARIES

The interaction of radiation with matter is through scattering and absorption. Absorption of photons , during their passage through matter results in attenuation of the beam. This property is used in reconstruction of the density profiles of the two-phase flow.

Single beam mono-energetic radiation phenomenon in a plane is represented by

$$N = N_o \exp\left[-\int_c \mu(r,\phi)\,dl \right]. \qquad (1)$$

The value of μ is characteristic of the material and also depends on the energy of the incident radiation. Eq (1) considers μ to be a two-dimensional function of position, as the path of radiation is assumed to be restricted to a plane. For monochromatic radiation the energy dependence of μ is not of concern. For a cross-section of interest, having non-uniform distribution of 'μ', equation (1) reduces to

$$p = \ln(N_o/N) = \int_c \mu(r,\phi)\,dl \qquad (2)$$

Radon [1] showed that it is possible to recover μ from a set of several p-values measured along various chords, c. If desired, these μ-values can be suitably calibrated to give the density values. This property is utilized in estimating the void-fraction in a two-phase flow.

2.1 DATA COLLECTION MODES

Data collection in tomography defines to a considerable extent, the speed of the reconstruction and the complexity of the reconstruction algorithm. The main modes in data collection are the parallel beam-geometry and the fan-beam geometry [8].

2.1.1 PARALLEL-BEAM GEOMETRY

In this mode there are several pairs of radiation source and detector systems which scan the object completely. As shown in Fig.1, the source - detector pairs are spaced uniformly and the object to be imaged is stationed on a rotating table to give different values of θ. The line SD represents the path of the data ray. The perpendicular distance of the ray from the origin is denoted by s. Several SD pairs collect the data p for a given θ. This set of p is known as a 'projection', which are collected for different views (at different θ). This data is denoted by $p(s;\theta)$.

2.1.2 FAN-BEAM GEOMETRY

In this mode, a single source is viewed by several detectors, simultaneously. The source angle is denoted by α and the detector angle by β. The readings are taken at differen values of β to get the data, denoted by $g(\alpha,\beta)$ or $h(\lambda,\beta)$. Here, is the perpendicular distance from the origin to the particula ray. This configuration, depicted in Fig.2, is widely used i

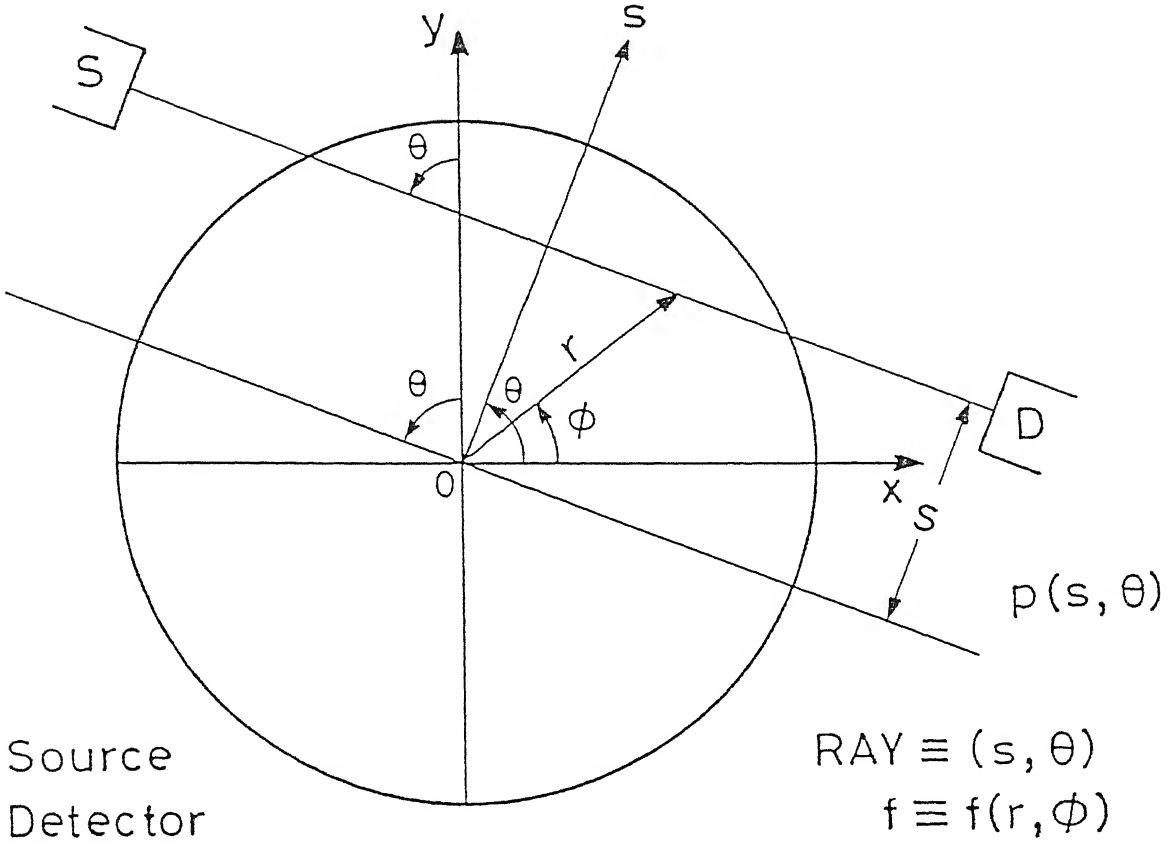

Fig. 1 Parallel beam collection geometry.

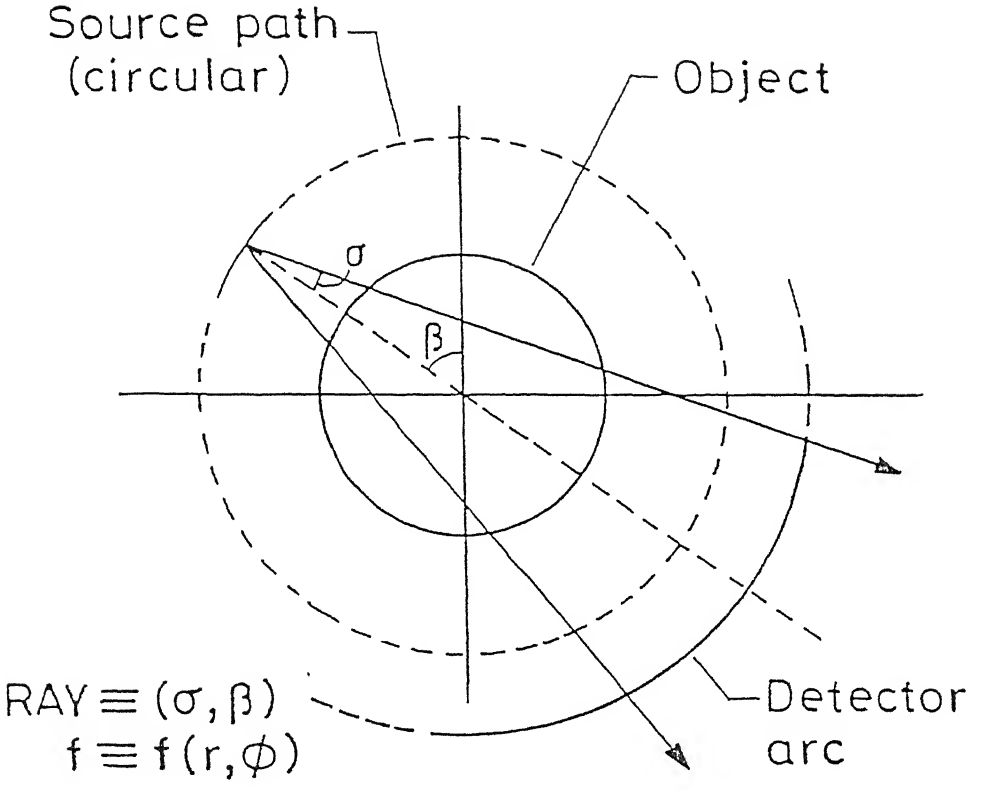

Fig. 2 Fan-beam data collection geometry.

tomography for medical purposes.

2.2 MATHEMATICAL FORMULAE FOR TOMOGRAPHIC INVERSION

Tomographic inversion methods are generally categorised as the 'transform methods' and the 'algebraic reconstruction techniques'. The transform methods are based on mathematical formulae while the latter are iterative computational techniques. In the following sections, "transform" methods are briefly summarised for the two data collection geometries.

2.2.1 PARALLEL BEAM FORMULATION

The reconstruction process of a two-dimensional function from its projections (line integrals) involves Fourier transforms for parallel beams and Hilbert transforms for divergent beam data. A very convenient transformation from FBG to PBG avoids the use of the Hilbert transform. The 'central-slice' theorem (also called the projection theorem) states that the one dimensional Fourier transform of the projection data, $p(s;\theta)$, with respect to the first variable s,is equal to the two-dimensional Fourier transform of the object function f. Mathematically,

$$\hat{f}(F;\theta) = \hat{p}(F;\theta) \qquad (3)$$

Taking the inverse Fourier transform of (3) we get

$$f(r,\phi)=\int_0^{\pi}\int_{-\infty}^{\infty} p(F;\theta)\exp[-i2\pi Fr\cos(\theta-\phi)]|F|\,dF\,d\theta \qquad (4)$$

For a given θ,

$$\hat{p}(F;\theta) = \int_{-R}^{R} p(s;\theta)\exp[-i2\pi Fs]ds. \qquad (5)$$

Equation (4) requires continuous projection data for all values of s and θ. For computational feasibility, a filter function is incorporated in the Fourier domain, to enable a finite cutoff frequency. This necessity arises because the limits on R vary from $-\infty$ to $+\infty$, which introduces divergence. This filter function, W(F), vanishes for $|F|$ greater than A, the cut-off frequency. Eq (4) is transformed to

$$f(r,\phi) = \int_{0}^{\pi} \int_{-\infty}^{\infty} p(F;\theta)\exp[-i2\pi Fr\cos(\theta-\phi)]W(F)|F|dFd\theta \qquad (6)$$

The reconstruction is approximate as all the higher frequencies have been eliminated. Besides, as per the sampling theorem, the cut-off frequency and the sampling interval in the spatial domain are related by

$$A \geq [1/(2\Delta s)] \qquad (7)$$

where Δs is the spacing between the rays.

The band-limiting filter, introduced in electron micrography by Ramachandran & Lakshminarayan [4] is given by

$$W(F) = \begin{cases} 1, & |F| < A \\ 0, & |F| \geq A \end{cases} \qquad (8$$

The sinc filter used by Shepp & Logan [9] is given by,

$$W(F)= \begin{cases} \sin[(\pi F/2A)]/(\pi F/2A) & ,|F|<A \\ 0 & ,|F|\geq A \end{cases} \qquad (9)$$

The filter used in this thesis is the Ramachandran & Lakshminarayan filter mentioned earlier.

2.2.2 FAN-BEAM FORMULATION

The inversion formula for the FBG case was first derived by Herman and Naparstek (1978) and is given by,

$$\tilde{f}(r,\phi) = (1/4\pi^2) \int_0^{2\pi} \int_{-B}^{B} (1/\sin(\sigma'-\sigma))\, D_v\, g(\sigma,\beta)\, d\sigma\, d\beta \ , \qquad (10)$$

where, D = distance of source from reference origin,

σ = angle of the data-ray with the reference ray,

B = angle of the extreme data rays,

β = source position,

$g(\sigma,\beta)$ = data for the ray represented by (σ,β),

$D_v\, g(\sigma,\beta) = (1/U)\left[\frac{\partial g}{\partial \sigma} - \frac{\partial g}{\partial \beta}\right]$,

$\sigma' = \tan^{-1}[(r\cos(\beta-\phi))/(D+r\sin(\beta-\phi))]$,

$U = [(r\cos(\beta-\phi))^2 + (D+r\sin(\beta-\phi))^2]^{1/2}$,

and the remaining variables are same as for the PBG case (see Fig.1). In the above equations U is the distance of the radiation source from (r,ϕ) ,the point being reconstructed ,and σ' is the angular displacement of the particular data ray passing through that point (r,ϕ). A major difference (compared to Eq.(6), which derives the reconstruction formula for parallel beam geometry) is the computation of partial derivatives of the data, g.

For FBG instead of using the formula derived by Herman & Naparstek, we used the transformation [10],

$$l = \frac{\lambda}{\sqrt{1 + (\lambda/D)^2}}, \quad \theta = \beta + \tan^{-1}(\lambda/D)$$

That is,

$$h(\lambda,\beta) = h\left(\frac{1}{\sqrt{1 - (1/D)^2}}, \quad \beta = \theta - \sin^{-1}(1/D) \right) \equiv p(l,\theta) \qquad (11)$$

where β denotes the source angle and λ denotes the perpendicular distance from the origin to the particular ray from the source. In Fig.3, this conversion has been graphically depicted.

2.3 CONVOLUTION BACK-PROJECTION ALGORITHM

Reconstruction algorithms based on the inversion formulae are called 'transform methods' [8]. They are slow and require accurate interpolating schemes in computing the two-dimensional inverse Fourier transform. The introduction of convolution [2, 4] eliminated the use of the Fourier transform and its inversion.

For PBG , equation (4) can be written as

$$f(r,\phi) = \int_0^{\pi} \int_{-R}^{R} p(s;\theta) q(s'-s)\, ds\, d\theta \qquad (12)$$

$$q(s) = \int_{-A}^{A} W(F)|F| \exp(i2\pi Fs)\, dF \qquad (13)$$

and $$s' = r\cos(\theta - \phi)$$

Here q is known as the convolving function and is th inverse Fourier transform of the function, $W(F)|F|$, where $W(F)$ i the filter function. The inner integral of eq (8) is a convolutio

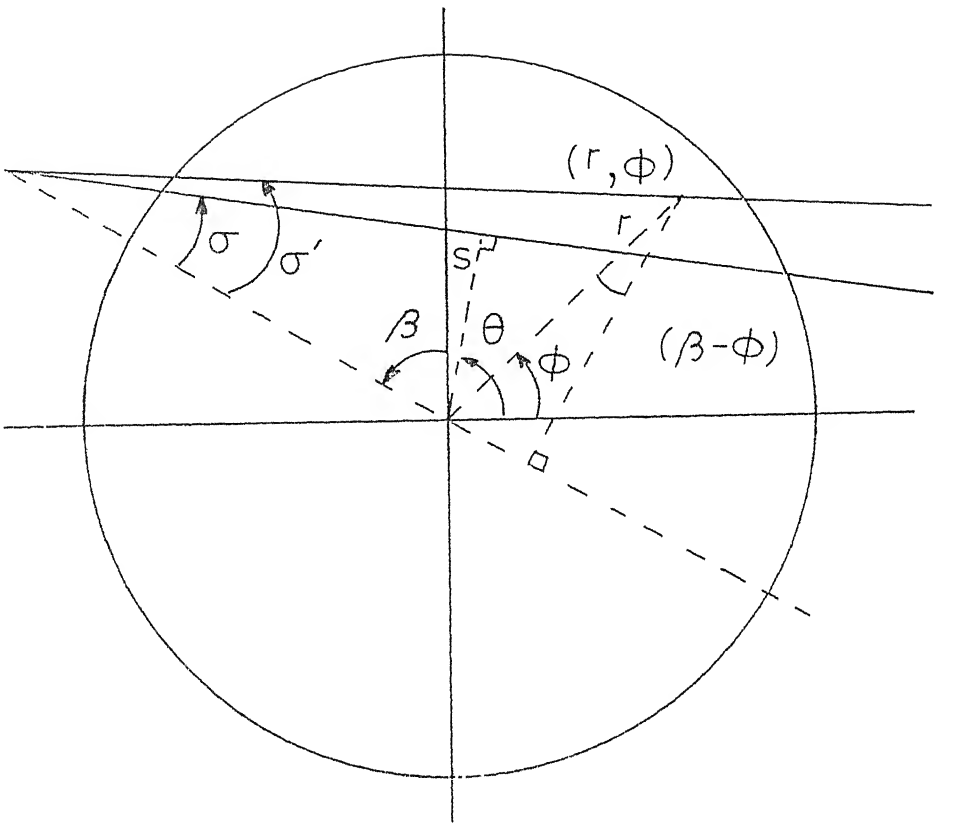

FIG. 3 CONVERSION OF FAN BEAM GEOMETRY TO PARALLEL BEAM GEOMETRY

and the outer integral is called the back-projection. The CBP algorithm is the most widely used method of reconstruction employed by commercial CT scanners used in the area of medical imaging.

2.4 AN OVERVIEW OF PHOTON STATISTICS

The quality of reconstruction is affected by the errors inherent to the data collection process itself. It is further affected by the discretization of the problem (that is, because, the number of projections is finite), and due to the errors by numerical computation. In this work, the errors due to photon statistics have been studied.

A very basic limitation to the accuracy of measurements taken in CT is the statistical nature of photon (whether gamma ray or x-ray) production, their interaction with matter and photon detection [11]. In gamma ray tomography, the rays are generally monochromatic, or at most, two distinct wave lengths are present. Due to this, the problems of uneven detector response to the detector, and of beam hardening, which plague x-ray tomography are mitigated [12].

If we consider that all the photons emitted by the source in a unit period of time in the direction of the detector are detected, the possible counts (which are non-negative integers) give rise to a discrete random variable denoted by Y. It can be further shown that the probability of occurrence of Y, at a specific value y is denoted by

$$P_Y(y) = \exp(-\Lambda)\Lambda^y / y! \qquad (14)$$

where Λ is a fixed real number

Eq (17) is called the Poisson probability law, and Y which satisfies this law is called a Poisson random variable with parameter Λ. The main properties of this variable are as follows :

a) its mean is Λ,

b) its standard deviation is $\sqrt{\Lambda}$

c) it behaves normally if Λ is large (>100).

To estimate Λ, which is the average number of photons emitted per unit time by a stable source (gamma ray or x-ray) in the direction of the detector, all the photons reaching the detector will have to be counted. Λ will be estimated by the count of the number of photons during a particular period of unit time (i.e. by a sample of the random variable). Poisson statistics imply that if we increase the sample by a factor of N, we reduce the size of the 1σ error by a factor of $\sqrt{N}$, where σ is the standard deviation.

The interaction of photons with matter also can be modeled as a discrete random variable. A photon leaving the source in the direction of the detector, will reach the detector (without being absorbed or scattered) with a fixed probability ψ. This probability depends on the energy of the photon and the material lying on the line between the source and the detector. ψ is called the transmittance of the material (along that particular line), at that particular energy. Of the photons which leave the source in the direction of the detector, a fraction ψ will eventually reach the detector, the rest being absorbed or scattered. The photons on reaching the detector are counted with an efficiency ε,

which is called the efficiency of the detector.

Thus the number of photons which actually reach the detector without being absorbed or scattered, and are counted by the detector is a sample of the random Poisson variable with parameter $\Lambda\psi\varepsilon$.

As discussed earlier,

$$-\ln\ (N/N_o) = \int_c \mu(r,\phi)dl \simeq m$$

where m is the ray sum and is the sample of a random variable such that,

$$|\ \mu_M + \ln(N/N_o)\ | < S$$

where

$$S \simeq (\phi_d \Lambda_a \psi_a \varepsilon_d)^{-1} \qquad (15)$$

and ϕ_d is the fraction of photons leaving in direction of the detector,

Λ_a is the number of photons emitted during the period of measurement,

ψ_a is the transmittance of the material and

ε_d is the efficiency of the detector.

CHAPTER 3

PROGRAM IMPLEMENTATION AND DESCRIPTION

There are various programs developed, in the course of this thesis work, which simulate the projected data, reconstruct images from actual or from simulated data and those which are used just to write or feed the data in a specified form. These programs have been written in FORTRAN. The program for simulating an error governed by Poisson statistics have been written in TURBO-PASCAL, by using the random number generation function available.

3.1 COMPUTER IMPLEMENTATION OF THE CBP ALGORITHM

The problem of reconstruction from projections is stated as follows :

Given $p(s;\theta)$, find $f(x,y)$.

In practice, the problem may be stated as :

Given discrete projection data in the form of estimates of p for a finite number of rays, find a 2-D distribution, which is a reconstructed estimate of the unknown object.

In the case when p is sampled uniformly in both s and θ, for N angles $\Delta\theta$ apart, with each view having M equispaced rays Δs apart, we define [8]

$$\left.\begin{aligned} M^{+} &= (M-1)/2 \\ M^{-} &= -(M-1)/2 \end{aligned}\right\} \text{ M odd}$$

$$\left.\begin{aligned} M^{+} &= (M/2)-1 \\ M^{-} &= -M/2 \end{aligned}\right\} \text{ M even}$$

In order to ensure that the collection of rays specified

by

$$\{(m\Delta s, n\Delta\theta): M^- \le m \le M^+, \quad 1 \le n \le N\}$$

covers the unit circle, we have,

$$\Delta\theta = \pi/N \quad \text{and} \quad \Delta s = 1/M^+$$

A reconstruction algorithm which can be implemented on the digital computer is required to evaluate $f_B(k\Delta x, l\Delta y)$, which is a band limited approximation of the function to be reconstructed. Here $K^- \le k \le K^+$ and $L^- \le l \le L^+$, where k and l are the positions of the co-ordinates of the image pixel. The definition of their upper and lower limits is similar to that of 'm'. Thus the projected data from N views and M rays is to be used to construct an image of K×L pixels. In this particular case ,the image is composed of 21×21 pixels from 18 views each having 21 rays. The back-projection integral is evaluated as follows :

$$f_B(k\Delta x, l\Delta y) \simeq \Delta\theta \sum_{n=1}^{N} \dot{p}(k\Delta x \cos\theta_n + l\Delta y \sin\theta_n, \theta_n) \qquad (16)$$

For each angle θ_n, the convolved values of $\dot{p}(s', \theta_n)$ for the K×L values of s' We can either have a separate convolution for every s' with the actual value of $q(s'-m\Delta s)$ at that point or we can evaluate $\dot{p}(m\Delta s, \theta_n)$ only within the specified limits of m and then use interpolation. The latter approach is much faster and cheaper. These operations are represented by

$$p_C(m'\Delta s, \theta_n) \simeq \Delta s \sum_{m=M^-}^{M^+} p(m\Delta s, \theta_n)\, q((m'-m)\Delta s), \qquad (17$$

$$M^- \le m \le M^+$$

$$p_I(s', \theta_n) \simeq \Delta s \sum_{m'} p_C(m\Delta s, \theta_n)\, I(s'-m\Delta s) \qquad (18)$$

where I(s) is an interpolating function. A linear interpolating function, say $I_L(s)$, corresponding to linear interpolation between adjacent samples is

$$I_L(s) = \begin{cases} \frac{1}{\Delta s}(1-|s|/\Delta s) & |s| \leq \Delta s \\ 0, & |s| \geq \Delta s \end{cases}$$

Using the above formulae , a program was written in FORTRAN to implement the CBP algorithm. Another program was written to simulate data for some standard functions [like f(r)= 1, r, exp(r), exp(-r), exp(3r) etc where r is the distance from the origin].

The data generated by the latter program was used to check the efficacy of the CBP program. Certain modifications were made in the CBP program to accommodate data obtained in the FBG. The mathematical basis of these changes is the FBG to PBG transformation mentioned earlier.

A calibration curve [density (ρ) versus attenuation-coefficient (μ)] was plotted using reconstruction results for water, pine, walnut and air (whose densities are known), after necessary corrections for the plexi-glass piping had been made. The CTN (Computer tomography numbers) for various two-phase flow situations were obtained. With appropriate normalization, the CTN and μ is identical. This normalization procedure, too, was included in the program. With the help of the calibration curve an idea about the point wise distribution of α is obtained. The density ρ and the void-fraction α, of a flow, are related by the expression

$$\alpha = 1-\rho$$

assuming the density of steam to be negligible.

To estimate the sensitivity of the CBP algorithm to the errors inherent to the data collected, an error with a Poisson distribution was deliberately introduced into the projection-data. This was done by using the random number generation function available in TURBO-PASCAL.

If N was the original count (projection-data), an error, which was a random number between $-\sqrt{N}$ and $\sqrt{N}$ was added to the original data.

$$N_{pol} = N + \text{random number}$$

where N_{pol} is the modified data

Errors for 2σ and 3σ deviation (where σ is standard deviation) were also generated, by simply multiplying the random number generated by a factor of 2.0 and 3.0 respectively.

3.2 PROGRAM FOR DATA SIMULATION

This program (see Appendix. B) computes the line-integrals of a given function between specified limits (in a bounded region). This program computes the line-integrals along parallel lines at equal distances from each other, for a number of views. The various steps of the program are as follows :-

1) The parameters of the program like the upper limit (B), the lower limit (A), the number of divisions (D), the slope (M) of the line and its intercept (C) are read from a data file.

2) The given function is incorporated in an appropriate form into the program.

3) The line integral of the above function is computed by using Simpson's one-third rule. Since it is path dependent, the integration rule has to be appropriately modified. A subroutine has to be incorporated, to take care of the condition when the line is parallel to the Y-axis and its slope is infinite.

4) This whole process is repeated as many times as the number of views desired. The value of the intercept 'C' is changed during each iteration to ensure that the parallel lines along which the integrals are computed are equidistant from each other.

This program can be modified to simulate the data for a fan-beam geometry also.

3.3 PROGRAM FOR RECONSTRUCTING THE IMAGE FROM DATA

This program (see Appendix C) can reconstruct an image from either simulated data of Section 3.2, or experimental data. A program was written to accept simulated data for the parallel beam geometry and use it to reconstruct the image. Images of several standard functions were reconstructed within acceptable error limits.

This program was modified to accept data from the fan-beam configuration, by incorporating the transformation mentioned by Kwoh et al [10]. The salient feature of this program, not found in [9] (which has reconstruction program for PBG), was to display the reconstructed image as every view was convolved and back projected.

A suitable image quality index would be helpful in quantitatively estimating the accuracy of image reconstruction.

Two such indices are l_1 and l_2 [13]. The process of reconstruction can be terminated if the error of reconstruction reaches a certain minimum value . Another index which has shown promising results is the " fractal dimension " [14]. The actual program details are as follows:

1) The parameters of the program like NDIV (the number of rays in a view) and NVIEW (the number of views) are read in from a data file. For fan-beam data the corresponding parameters will be the source to detector distance (D), the radius of the object (RAD), the number of projections in a scan (NRAY) and the number of scans (NVIEW).

2) The projected data are read in from a data file. If the data values are for a fan-beam geometry then the transformation of co-ordinates from fan-beam geometry to a parallel beam geometry was done.

This transformation enables us to use the CBP algorithm, for fan-beam data, without resorting to the Hilbert transform.

3) The Ramachandran-Lakshminarayan filter was used in this program. The numerical values had been computed and stored in a file. These values were merely read from the file into an array. It is at this stage that the convolution is carried out.

Convolution is especially easy if the values to be convolved are stored in an array.

It is often found that, during back-projection of data, the convolved values do not exactly pass through the point being reconstructed. Due to this interpolation has to be used. Since linear interpolation is fast and it gives good results, it has been used in this particular implementation.

4)The superimposition (backprojection) of these interpolated values is carried out. Some conveniences like display of point values as they are reconstructed have been added to the program. These reconstructed values are the LITF values.

A sample output of this program has been displayed in Appendix E.

3.4 PROGRAM TO INCORPORATE RANDOM ERRORS INTO THE DATA

This program (see Appendix D) has been written in TURBO-PASCAL. It utilises the random number generating function available in the TURBO-PASCAL library.

For a Poisson distribution with mean 'N', the standard deviation is given by $\pm\sqrt{N}$. A random number with a maximum absolute value of $+\sqrt{N}$ is generated. This quantity is superimposed on the experimental data, in effect simulating a Poisson distribution for the inherent statistical variations.

CHAPTER 4

RESULTS AND DISCUSSIONS

In this chapter, the results obtained with the actual experimental data have been discussed.

4.1 DATA USED

The data used was taken from the study conducted by Munshi [15]. The details are briefly summarized as follows:-

a) The source of nuclear radiation was 13.86 mCi of Cs-137. The collimator fixed at the other end was rotated through an angle of 50° (25° on either side).

b) The detector was connected to this, the subsequent stages being a preamplifier, an amplifier, a baseline restorer, a single channel analyser and a timer.

c) The data collected for calibration was for water, air, walnut and pine. The air-water bubble column was used to measure densities by reconstruction tomography.

These calibration quantities have been listed in Table 1.

4.2 DISCUSSION OF THE RESULTS

The results of the investigations are presented in Fig.4-15 and Tables 3-5.

The reconstruction results given in Fig.5-15 have been labelled using the following convention

1) T denotes two-phase flow.

2) The second numeral (10 to 40) denotes the cross-sectionally averaged void-fraction in that particular case.

3) The alphabet has been used for distinguishing apart the different cases, and is connected to the different case numbers. No alphabet has been used to denote the first case.

4)The last numeral (0, 1, 2 or 3) denotes the magnitude of the error, as a multiple of σ.

Expression (15) in section 2.4 shows that the error in measurements depends on various different factors and it may be reduced by

1) Increasing the strength of the source or the time period of measurement and thus ϕ_d.

2) Improving the efficiency of the detector.

In Fig.4, the relationship between LITF and ρ (density) for known materials has been graphically depicted. It is a linear relationship and has been used as a calibration curve for cases where LITF is known and ρ(density) or α(void fraction) is unknown. Thus, with the help of Fig.4, further investigations have been carried out, regarding the deviation in density or void-fraction, by relating it to the change in the value of LITF.

The cases of two-phase flow investigated are listed in Table 2.

The projections for the calibration quantities are assumed to be relatively less affected by statistical errors since averaging over a large number of readings has been carried out. In Fig.5, the reconstructed profiles for these materials, along the largest chord (i.e. the diameter) have been plotted. Fig.6-9 show the reconstructed profiles for case 1 with errors from 0 to 3σ.

These have been reconstructed for $\langle\alpha\rangle$=0.1 to 0.4. For an error larger than 1σ, the error in reconstruction is very large (up to 60.0 %). But, from the Poisson statistical curve, we know that about 99% of the random variables lie within a range of $\pm 3\sigma$ from the mean for that particular distribution. Thus, if we have a reconstructed profile, from data within a broad band of 'true counts $\pm 3\sigma$ ', the reconstructed profile also occupies a 'band'. The degree of confidence in the reconstruction band increases as we increase the range in which the detector counts may lie.

Various other observations can be made on the basis of Table 3 and the radial profiles plotted in Fig 10-15. It is seen that the deviation due to the error incorporated is minimum at the edge of the reconstruction and increases towards the centre. The deviation is maximum at the centre of the reconstruction for all the cases. These values of maximum deviation have been listed in Tables 3- 5. Table 3 depicts the deviation at the centre as a percentage of the central pixel value in the original reconstruction (i.e. without any error incorporated). Table 4 depicts the differences between original pixel value and the values with the error incorporated. Table 5 depicts the deviation at the central pixel, for 2σ and 3σ errors.

If we consider only the magnitude of the deviation, in case 1, $\langle\alpha\rangle$=0.1 has a deviation of 17.64%, which increases to 21.94% for $\langle\alpha\rangle$=0.2 . For $\langle\alpha\rangle$=0.3, it reduces to 13.97% and again it increases to 34.73% for $\langle\alpha\rangle$=0.4 .

For case 2, $\langle\alpha\rangle$=0.1 has a deviation of 18.85%, which reduces to 18.26% for $\langle\alpha\rangle$=0.2 .It further reduces to 13.85% for $\langle\alpha\rangle$=0.3 and then it increases to an all time high of 42.93% for

TABLE 1

CALIBRATION TABLE

Sr.no	Material	LITF	Density
1	AIR	0.0000	0.0 g/cm^3
2	PINE	0.0833	0.41 g/cm^3
3	WALNUT	0.1480	0.73 g/cm^3
4	WATER	0.2205	1.00 g/cm^3

TABLE 2

CASES INVESTIGATED

Void fraction $\langle\alpha\rangle$	Density g/cm^3
10%	0.9
20%	0.8
30%	0.7
40%	0.6

TABLE 3

TABLE OF DEVIATION AS A PERCENTAGE

Sr.no	DEVIATION (%)			
	$\langle\alpha\rangle$=0.1	$\langle\alpha\rangle$=0.2	$\langle\alpha\rangle$=0.3	$\langle\alpha\rangle$=0.4
1	17.64	-21.94	13.97	34.73
2	18.85	-18.26	13.85	42.93
3	18.98	-13.96	-24.05	33.48
4	18.21	-19.20	-25.77	1.73
5	-19.16	18.06	-25.95	31.64
6	18.82	-19.99	16.84	41.96

TABLE 4

ABSOLUTE DEVIATION OF DENSITY

Sr.no	DEVIATION			
	$\langle\alpha\rangle$=0.1	$\langle\alpha\rangle$=0.2	$\langle\alpha\rangle$=0.3	$\langle\alpha\rangle$=0.4
1	0.1436	-0.1734	0.0897	0.1870
2	0.1649	-0.1374	0.0854	0.2059
3	0.1595	-0.0923	-0.1402	0.1305
4	0.1711	-0.1422	-0.1488	0.0085
5	-0.1391	0.1128	-0.1430	0.1298
6	0.1704	-0.1474	0.1131	0.2086

TABLE 5

ABSOLUTE DEVIATION OF DENSITY FOR 2σ and 3σ ERROR FOR CASE 1

$\langle a \rangle$	DEVIATION	
	2σ	3σ
0.1	0.0690	0.1063
0.2	-0.0696	-0.1005
0.3	0.0454	0.719
0.4	0.0868	0.1323

α=0.4 .

In case 3, α=0.1 has a deviation of 18.98% while α=0.2 has a deviation of 13.96% . This increases to 24.05% for α=0.3 and then it increases still further to 33.48% for α=0.4 .

In case 4, α=0.1 has a deviation of 18.21% while α=0.2 has a deviation of 19.20% . This increases to 25.77% for α=0.3 and then it reduces to 1.73% for α=0.4 .

In case 5, α=0.1 has a deviation of 19.16% while α=0.2 has a deviation of 18.06% . This increases to 25.95% for α=0.3 and then it increases still further to 31.64% for α=0.4 .

In case 6, α=0.1 has a deviation of 18.82% which increases to 19.99% for α=0.2 . This reduces to 16.84% for α=0.3 and then it increases to 41.96% for α=0.4 .

LITF, which is proportional to the point density, decreases logarithmically with 'N', as per eq (2), where 'N' is the number of counts, and is proportional to the number of photons reaching the detector. Therefore, as α increases, LITF should decrease in magnitude. This is because LITF is proportional to the density, it being a measure of μ, the attenuation coefficient. This implies that the magnitude of the deviation should increase with increasing α.

If we consider the magnitude of the deviation for α=0.1 and α=0.4, this trend is followed in 5 cases out of 6, case 4 being the sole exception. If, however, all the values of α are considered, then it is apparent that any explicit relation between the magnitude of the deviation and LITF cannot be readily inferred.This may possibly be due to a number of reasons.

Some of these are :

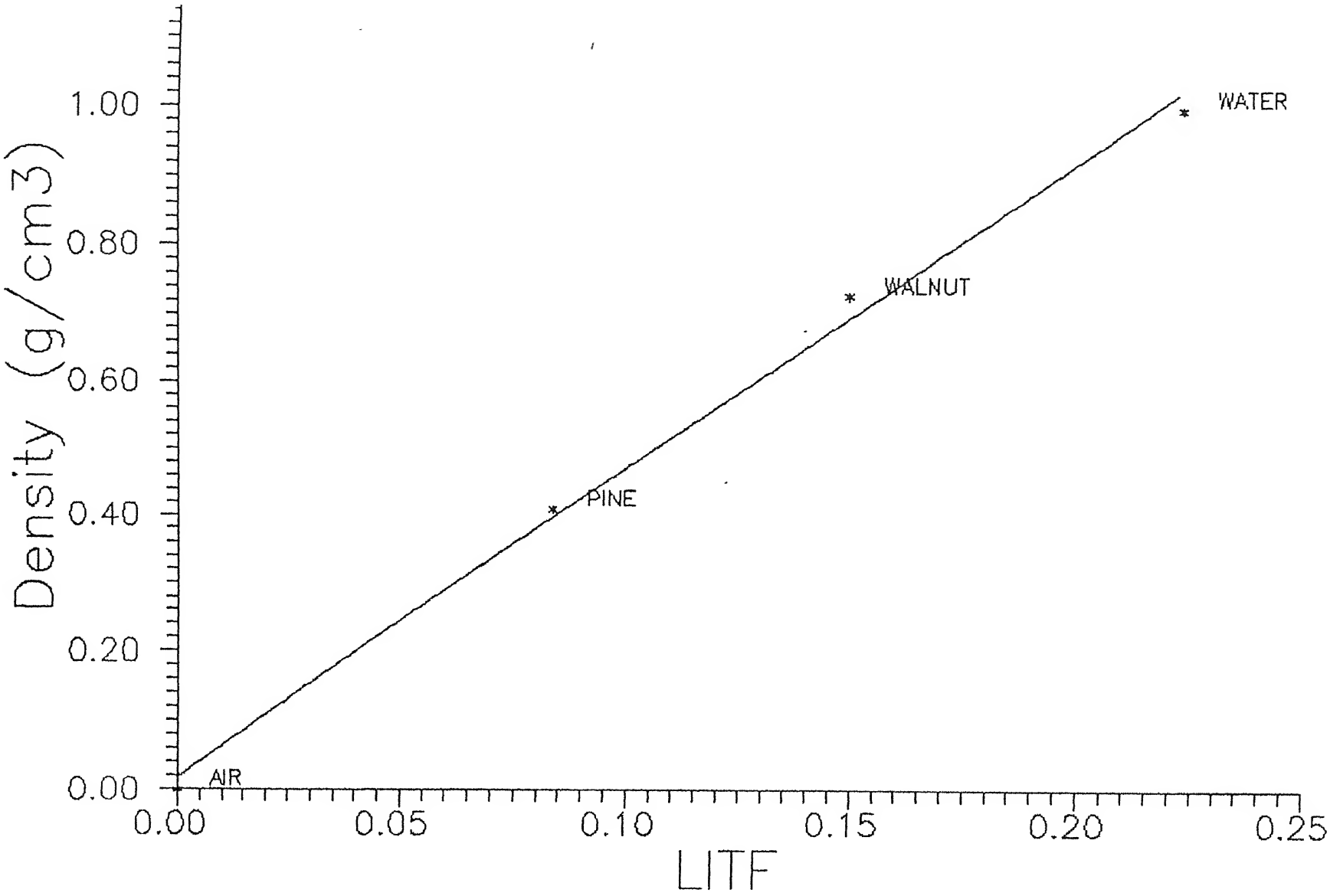

Fig. 4 : Calibration curve for case 1 to case 6.

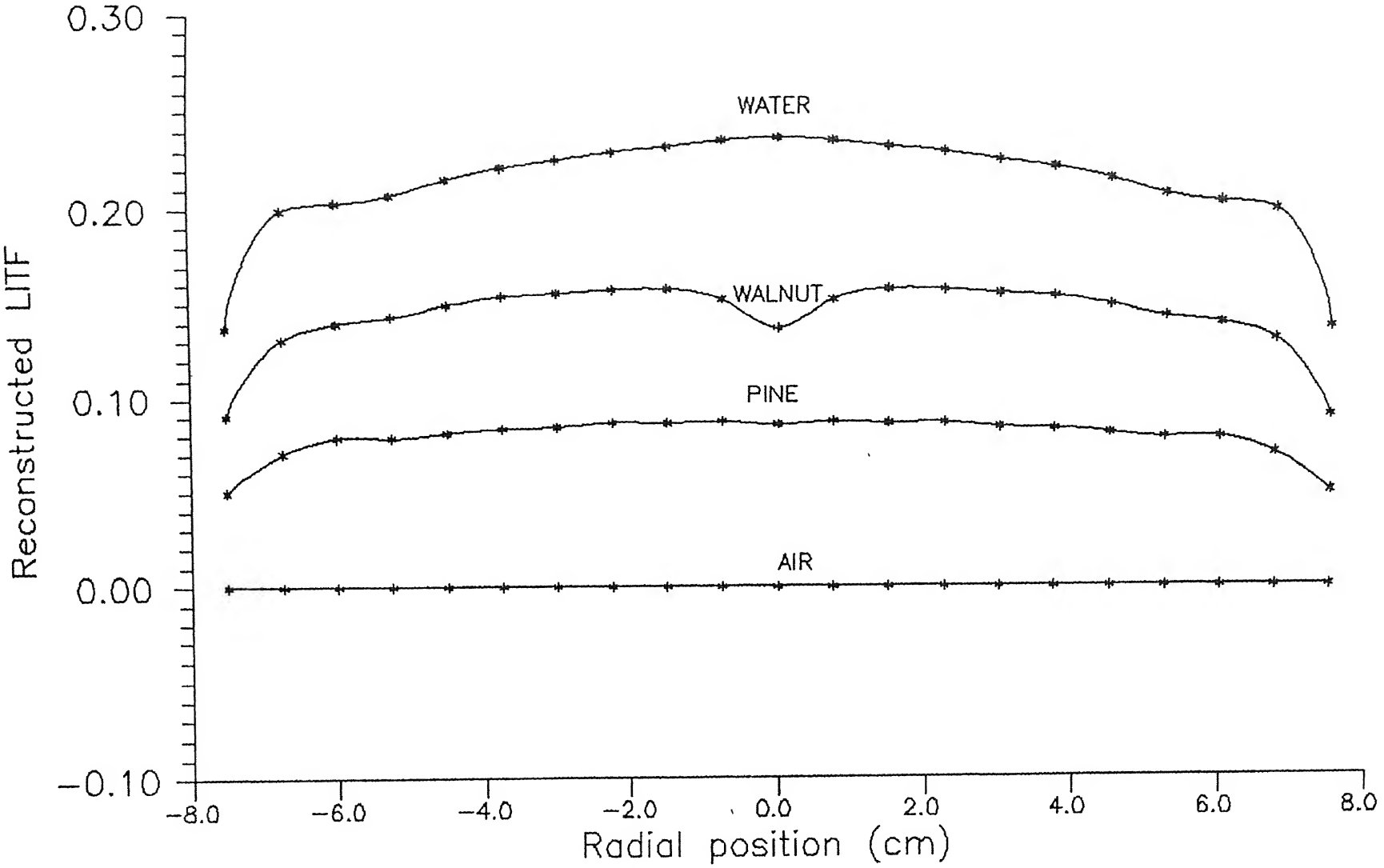

Fig. 5 : Reconstructed profiles for reference quantities.

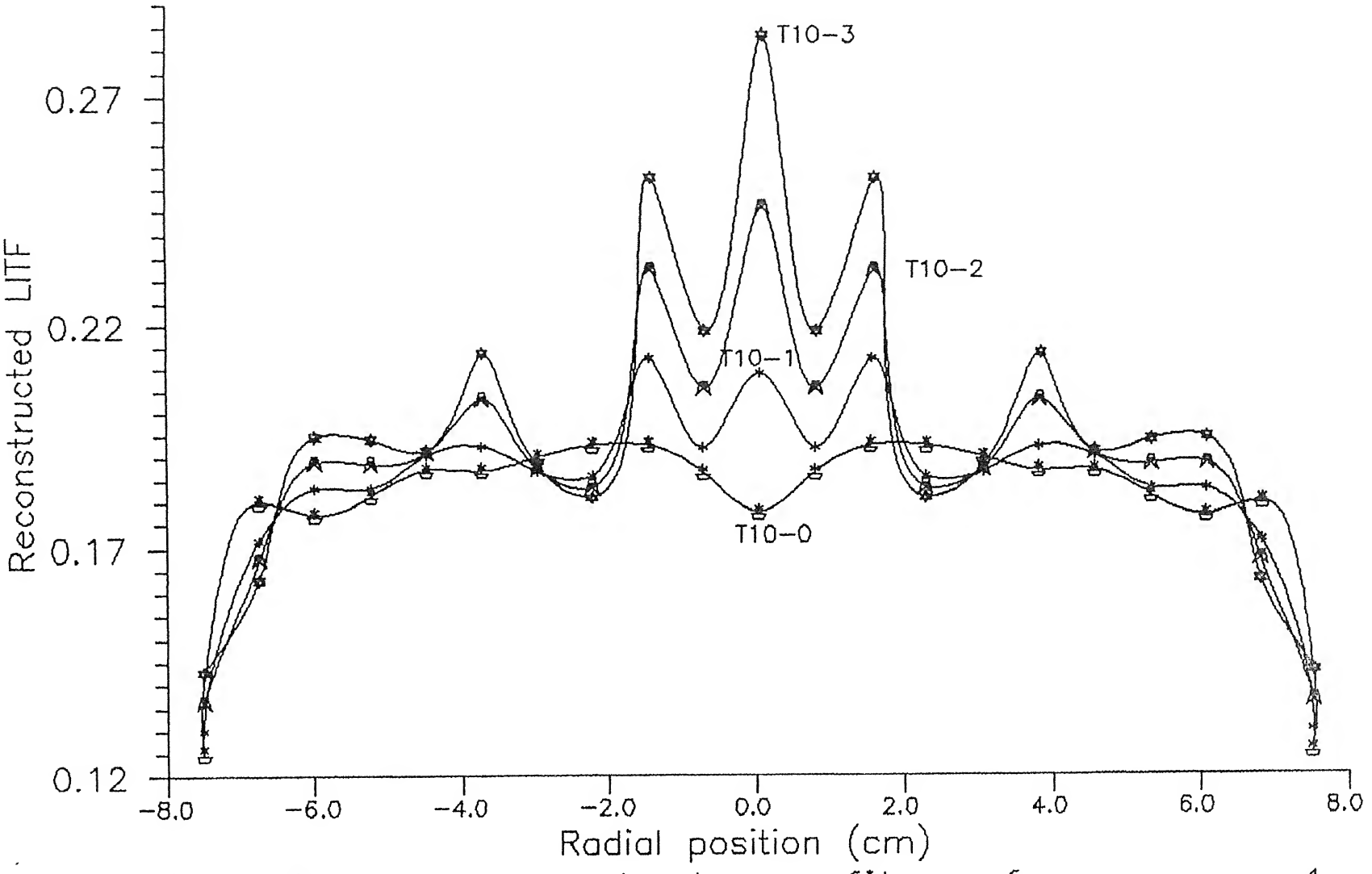

Fig. 6 : Reconstructed profiles for case 1 with 'alpha'=0.1 and error upto 3 'sigma'.

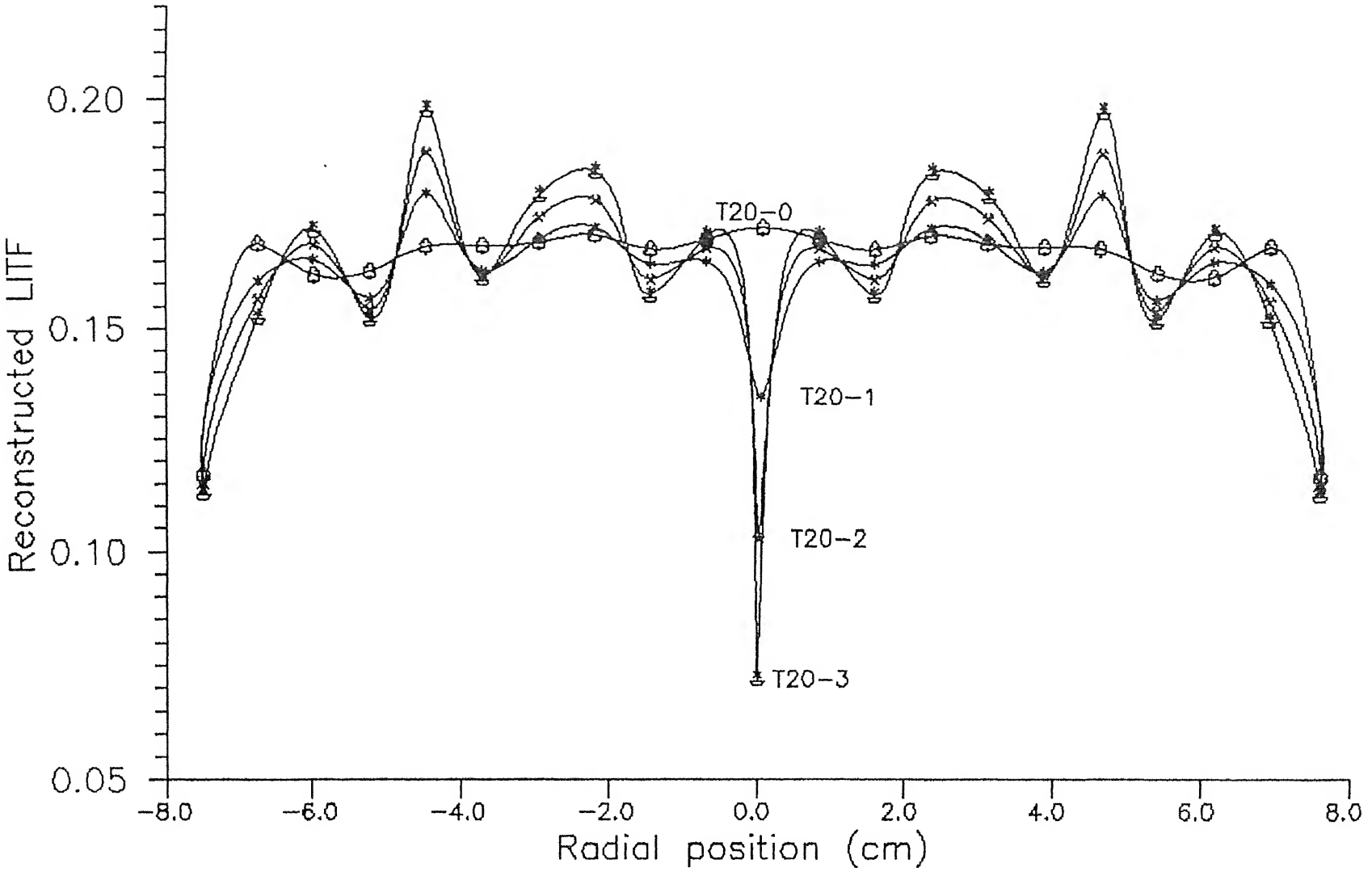

Fig. 7 : Reconstructed profiles for case 1 with 'alpha'=0.2 and error upto 3 'sigma'.

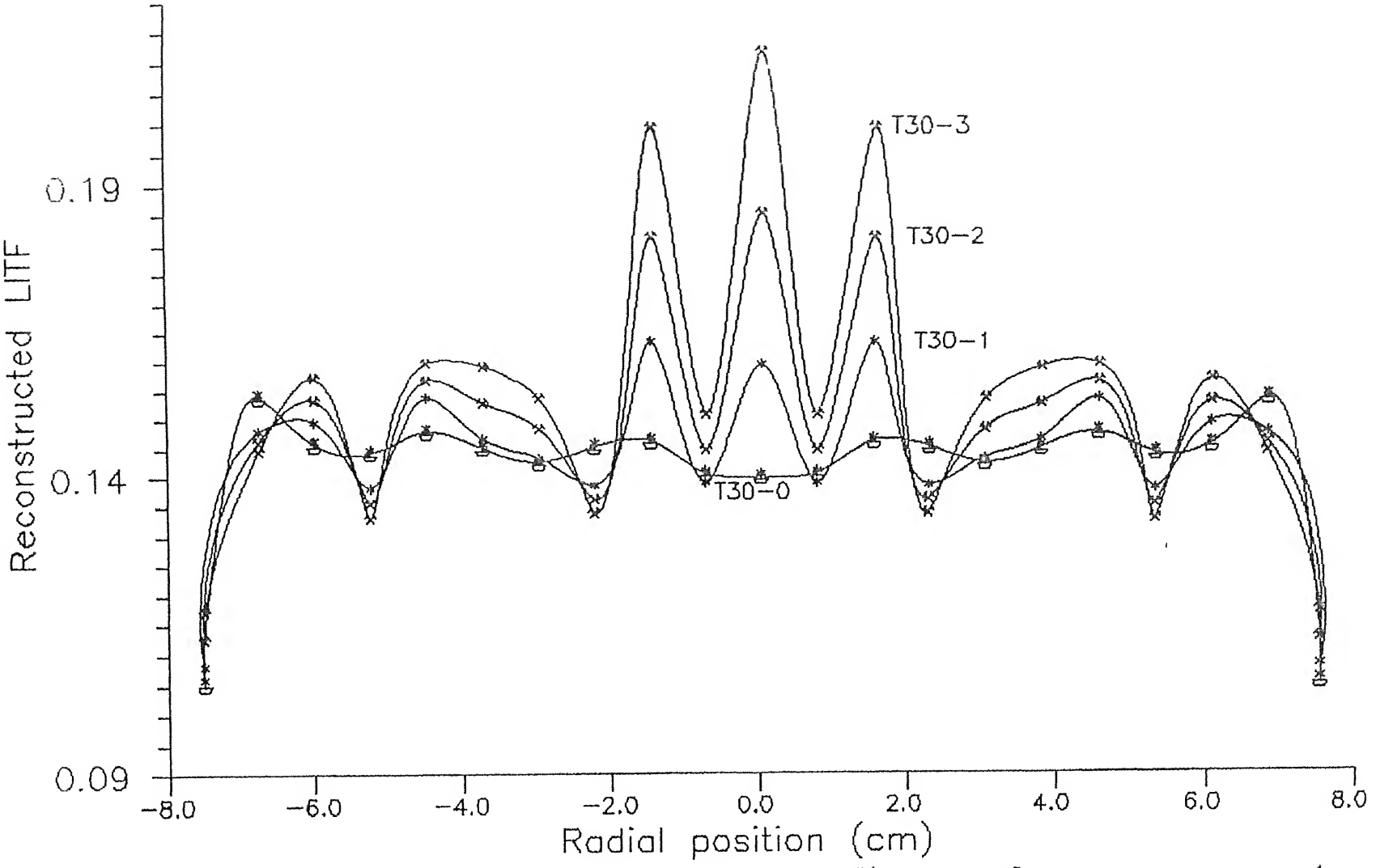

Fig. 8 : Reconstructed profiles for case 1 with 'alpha'=0.3 and error upto 3 'sigma'.

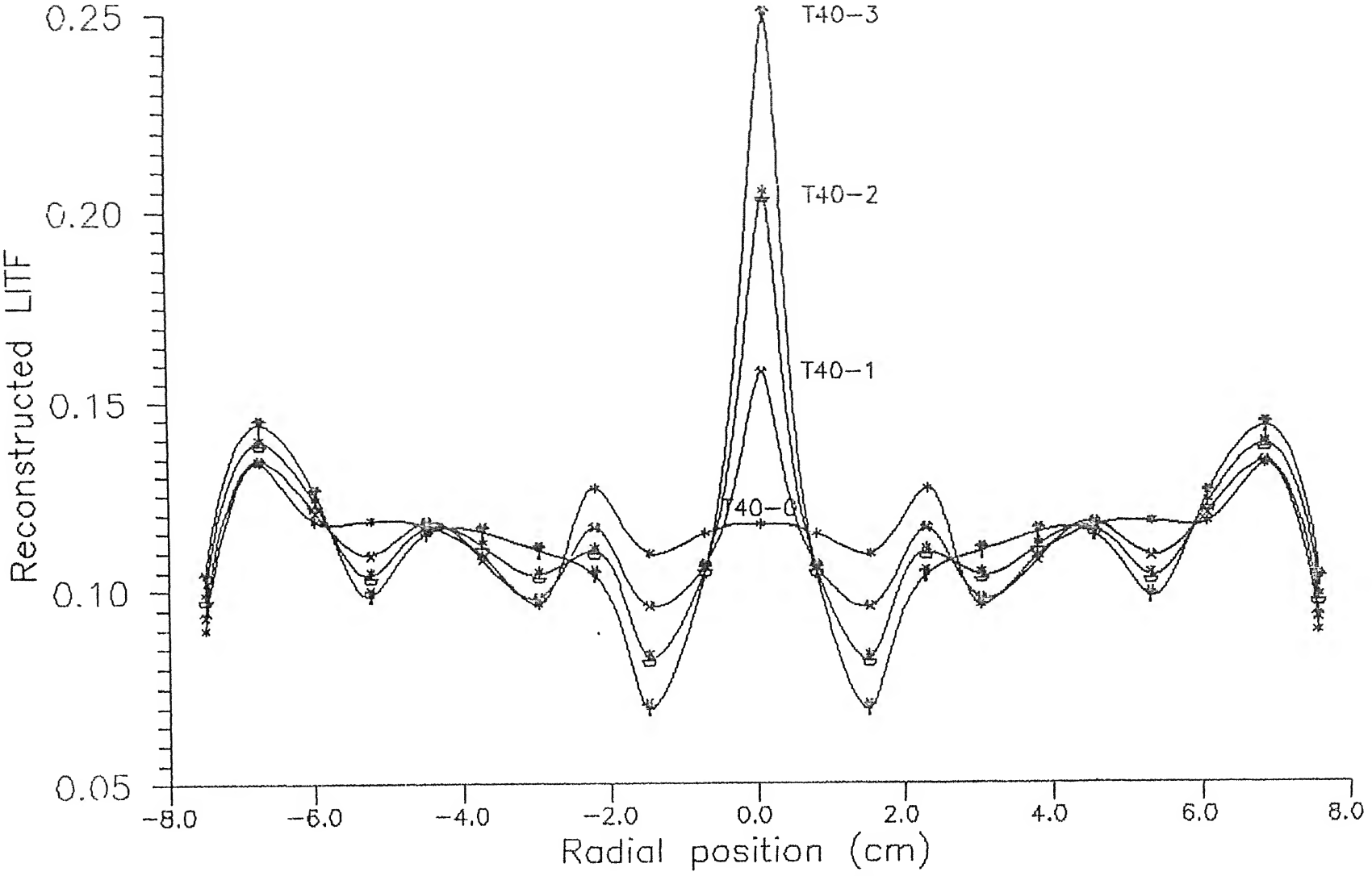

Fig. 9 : Reconstructed profiles for case 1 with 'alpha'=0.4 and error upto 3 'sigma'.

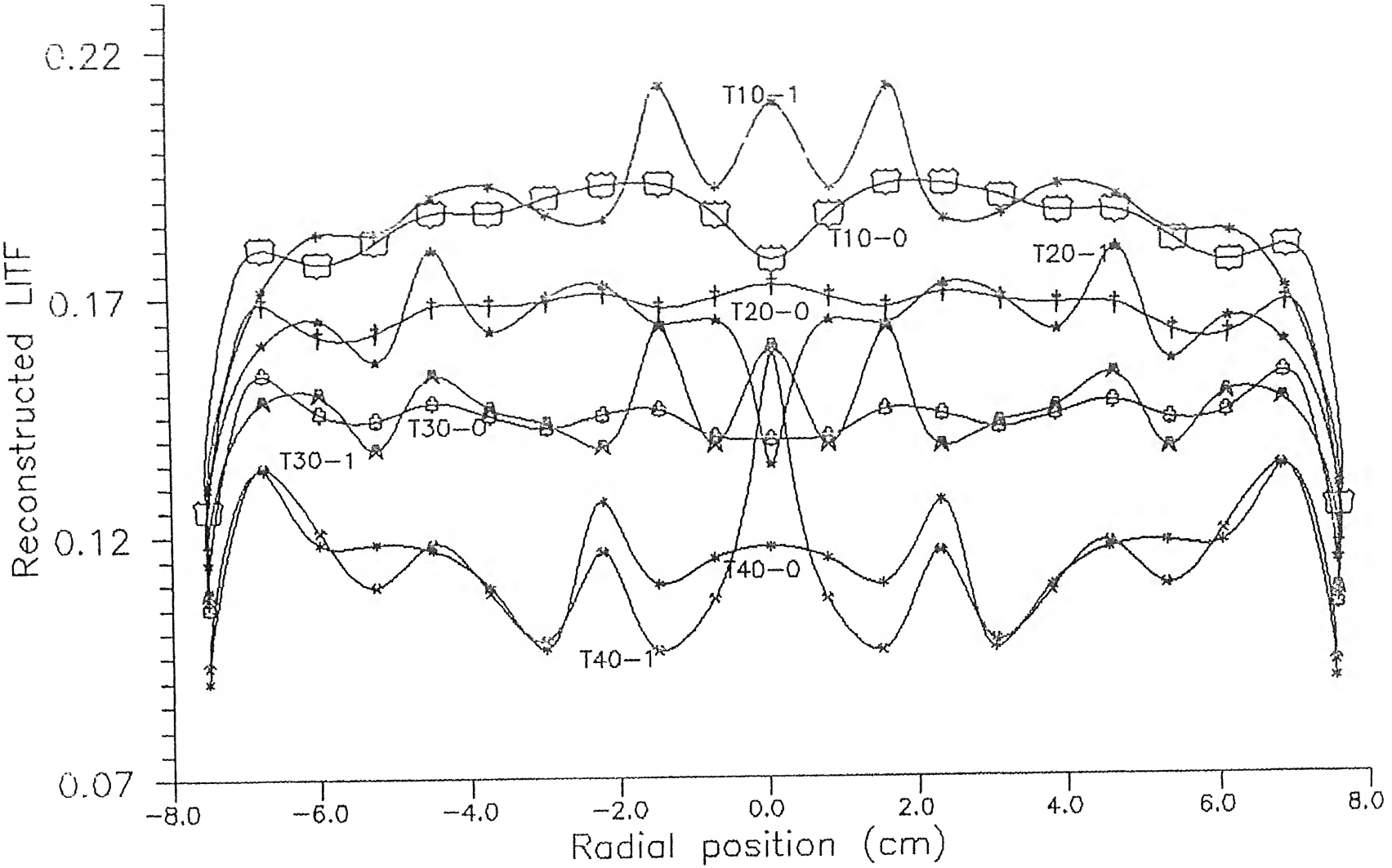

Fig. 10: Reconstructed profiles for case 1

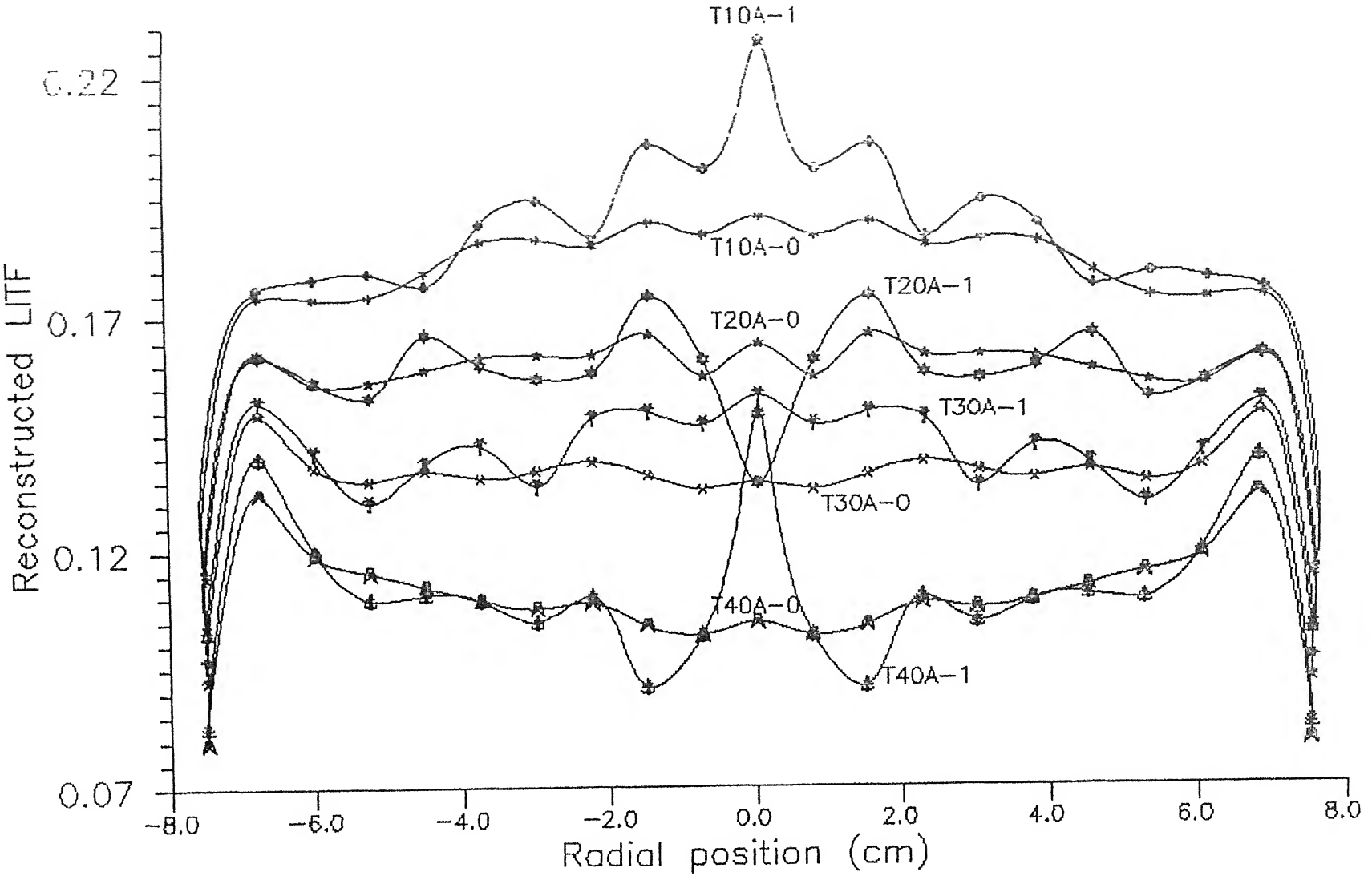

Fig. 11: Reconstructed profiles for case 2

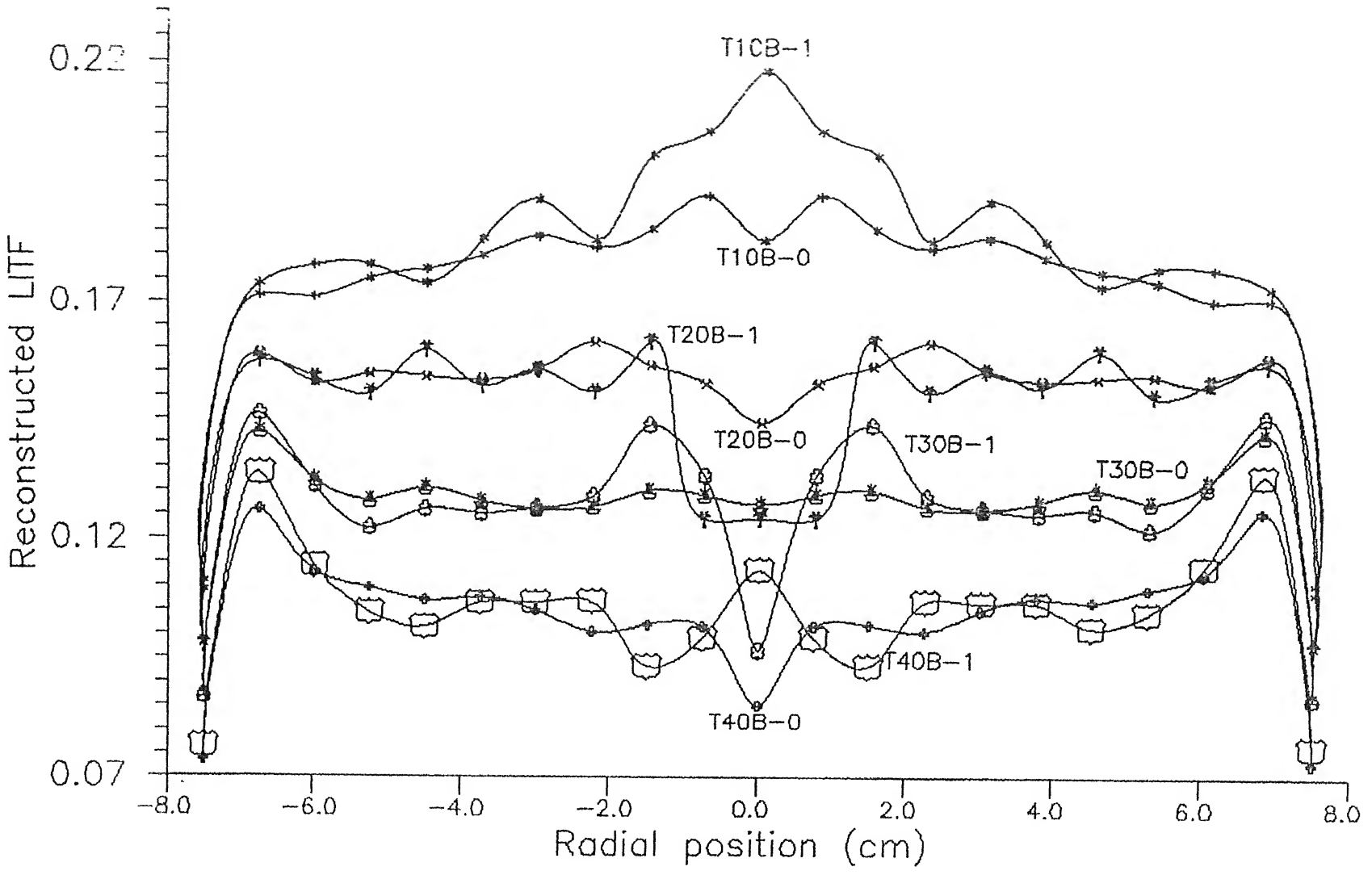

Fig. 12: Reconstructed profiles for case 3

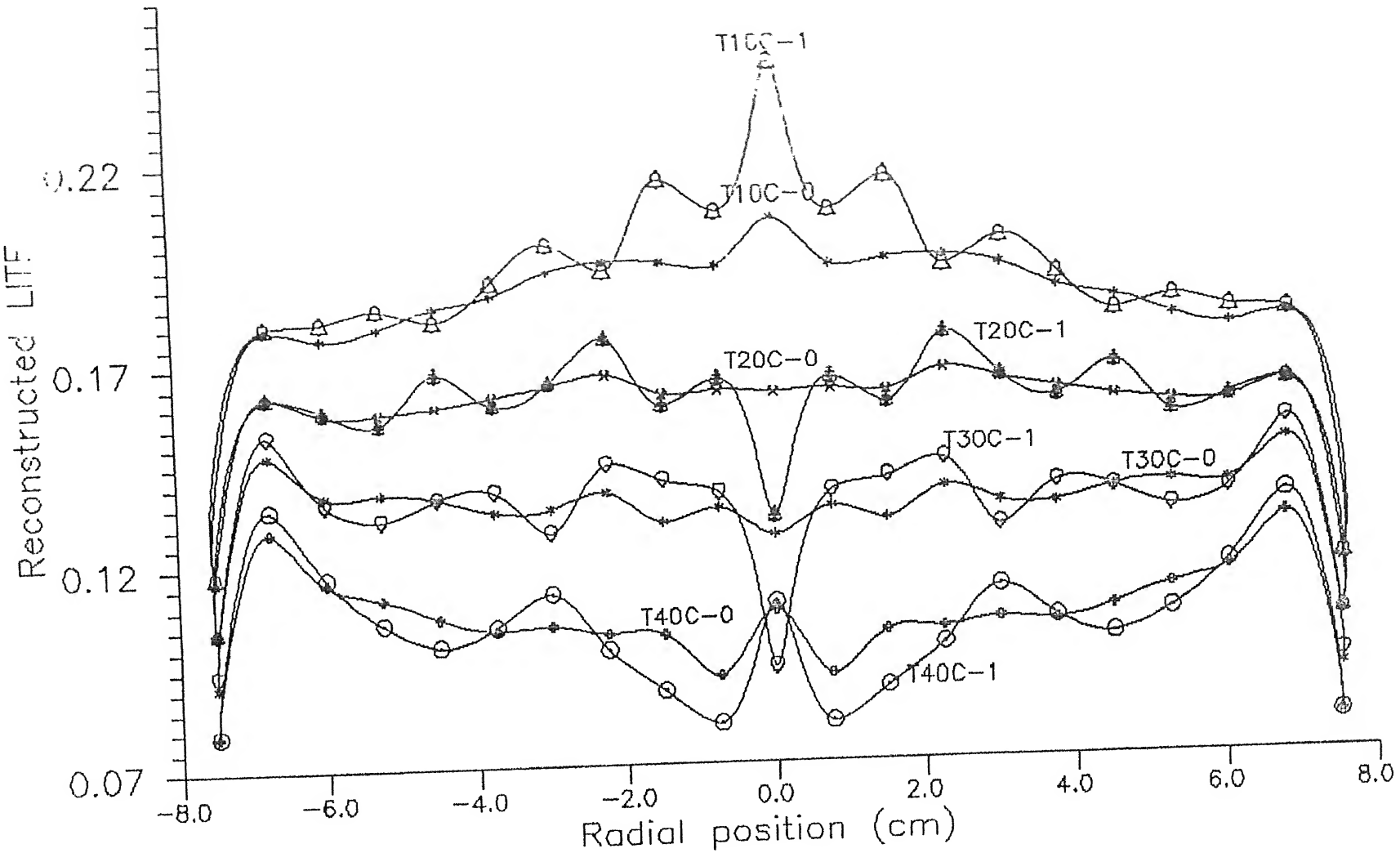

Fig. 13: Reconstructed profiles for case 4

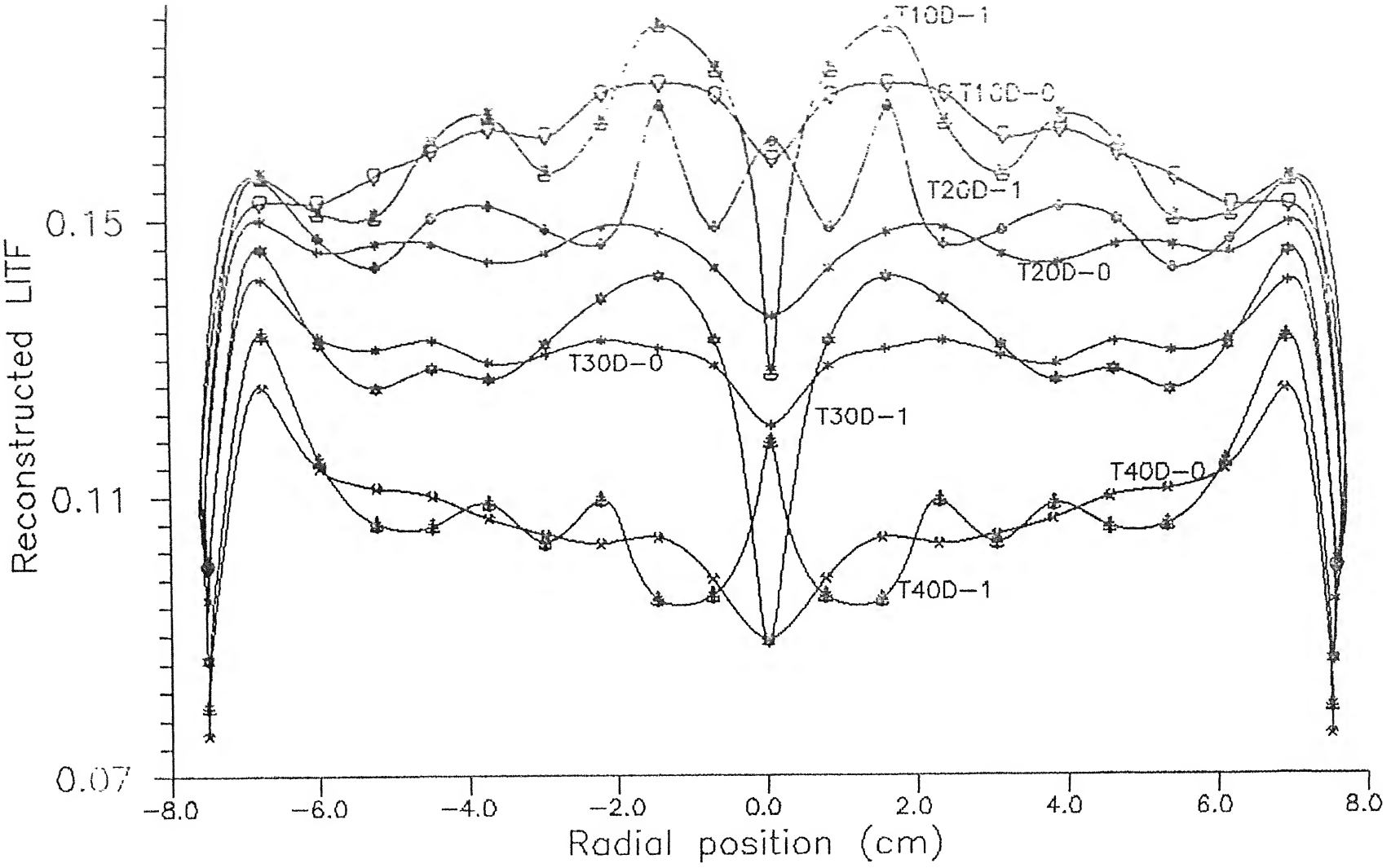

Fig. 14: Reconstructed profiles for case 5

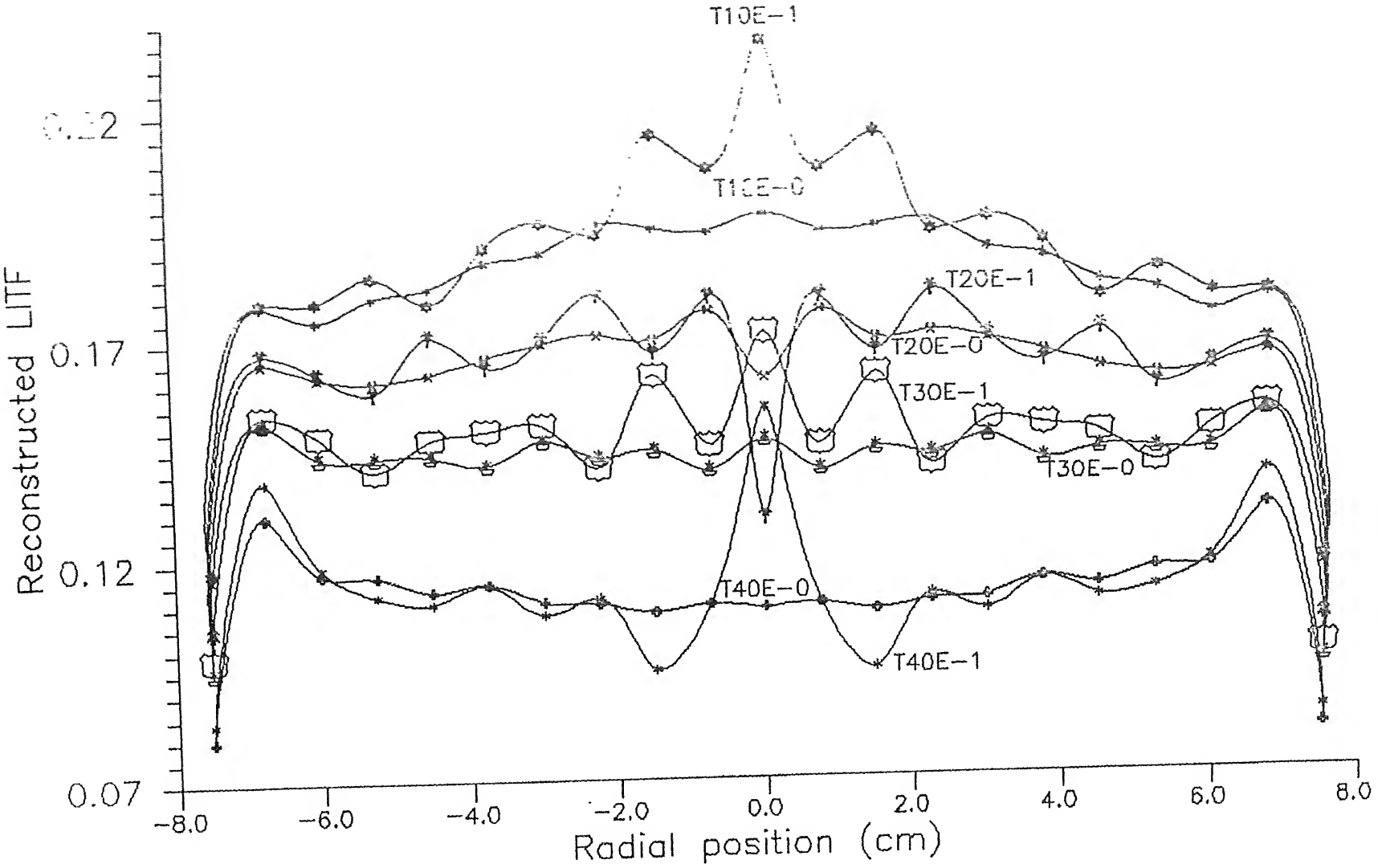

Fig. 15: Reconstructed profiles for case 6

1) Instead of the line integrals, we have strip integrals as the projection data. This is due to the finite source dimensions, leading to a finite, non zero beam width.

2) Values of LITF are averaged over the cross-section and calibrated using known density or void-fraction values, for corresponding values of $\langle\alpha\rangle$.

The detector for photon detection had been collimated to accept only those photons which come straight from the source. However, perfect collimation is difficult to achieve. This allows some scattered radiation to enter the collimator window, artificially boosting the counts. Since only straight attenuation photons are related to the chordal density, scattered photons produce an overestimate of the void-fraction, i.e an underestimate of the density (LITF). These effects due to photon scattering have not been taken into account. The increased number of counts due to scatter will not result in an overestimate of $\langle\alpha\rangle$ if the effect of scattered photons is the same along all chordal positions. This is a fairly strong assumption and may not be always valid. It has possibly resulted in underestimates of density (LITF), partially compensating for the greater effects of counting statistics at lower counts [15].

3) Due to the formation of bubbles, and their consequent collapse or liberation, the flow is said to be unsteady in the local sense, while being steady as a system since no mass accumulation occurs in the system. The bubbles generated are of different diameters and have different velocities. Due to these processes a "dynamic bias" error is inherent to the system. It is analogous to the "patient motion" errors encountered in medical

imaging and is an experimental error. Its manifestation is in t
form of streaking artifacts across the tomogram.

CHAPTER 5

CONCLUSIONS AND RECOMMENDATIONS

It has been observed in the course of study that the linear relationship between LITF and ρ (density) can be extended to get meaningful results for measurement of void-fraction in a two-phase flow. It is also possible to have LITF to be identical to μ, the attenuation constant of the material at that energy, by suitably normalizing the input data and ensuring that the same system of units is consistent during computation.

The error in reconstruction, due to the error incorporated in the projection data follows the predicted trend only for certain readings in a given set. This implies that, in addition to the effects of photon statistics, other errors like dynamic bias and counting of scattered photons are inherent to the projection data.

The sign of the maximum deviation is negative in about 35% of the reconstructions. But the reconstructed profile has no preference for sign for the individual pixels within a reconstruction. It is concluded that the statistical error has no preference for sign. It underestimates or overestimates the reconstructed values with almost the same frequency.

To reduce the error in reconstruction due to the statistical nature of photon behavior, the practical recourses are as follows :

1) Increase the number of detector counts (photons) by

using a source of higher strength. In medical applications, this would imply a higher radiation dosage, rendering this recourse unacceptable.

2) Use a low energy source for a longer interval of time, so that the effective mean counts are recorded due to the effects of temporal averaging. This would be acceptable only if the duration of measurement were substantially smaller than the duration of the fastest transient in the two- phase flow system.

It is apparent from the above recommendations that further investigations are needed along these lines. Besides, the study was conducted using only the Ramachandran- Lakshminarayan filter. Investigations for other window-functions, which are possibly less vulnerable to statistical variations can be carried out. The tomographic inversion has been carried out using limited amount of data. A larger number of views, as well as rays in a view will result in better results.

It is recommended to follow the courses mentioned above to investigate the effects of the statistical errors inherent to the data and consequently, to reduce these effects.

REFERENCES

1 J.Radon, "Uber die Bestimmung von Funktionen durch ihre Integralwerte längs gewisser Maanigfaltigkeiten", Berichte Sächsische Akademie der Wissenschaften Leipzig, Math.-Phys. Kl., 69 (1917), pp.262-267.

2 R.N.Bracewell, A.C.Riddle, "Inversion of Fan Beam Scans in Radio Astronomy", Astrophy.J.150, (1967) pp.427-434.

3 A.M.Cormack, "Representation of a Function by its Line Integrals with some Radiological Applications" J.Appl.Phys., 35 (1964), pp. 195-207.

4 G.N.Ramachandran, A.V.Lakshminarayan, "3-D Reconstruction from Radiographs and Electron Micrographs; Application of Convolution instead of Fourier Transforms", Proceeding. National. Academy. Science , USA, 68, 1971, pp 2236 -2240.

5 G.N. Hounsfield, "Computerized Transverse Axial Scanning Tomography : Part I, Description of the System" Br J Radiol., 46 (1973), pp. 1016-1022.

6 "CT Scans for Butchers", Science Today, 22, 3 (1988), p. 26.

7 W.H.Miller, "The Design of a Portable CAT Scanner for Utility Pole Inspection", Trans. American. Nuclear. Society (1986), 52, pp. 350-351.

8 R.M.Lewitt,"Reconstruction Algorithms: Transform Methods", Proc. IEEE, 71, No.3 (1983), pp. 390-408.

9 L.A.Shepp and B.F.Logan, "The Fourier Reconstruction of Head Section", IEEE Trans. Nucl.Sci., NS-21 (1974), pp 21-43.

10 Y.S.Kwoh, I.S.Reed, T.K.Truong and C.M.Chang," 3-D reconstruction for diverging X-ray beams ", IEEE Trans. Nucl.Sci., NS-25,No.3, June 1978, pp 1006-1014.

11 G.T.Herman, "Image Reconstruction from Projections : The Fundamentals of Computerized Tomography", Academic Press, New York (1980) .

12 A. Mackovski, "Physical Problems of Computerized Tomography", Proceedings of the IEEE, 71, No.3, (1983), pp 373-378.

13 P.Munshi, "Error Estimates for the Convolution Backprojection Algorithm in Computerized Tomography", Doctor of Philos Thesis, IIT Kanpur, (1989).

4 V.Bhatt, P.Munshi, and J.K.Bhattacharjee, "Analysis of the Performance of Medical CT Scanners Using Fractal Theory", Bulletin of Radiation Protection, 13, No.2, (1990), pp 38-40.

5 P.Munshi, "Two-phase Flow Studies in the Bubbly Flow Regime using a Scanning Gamma-Ray Densitometer", Master of Science Thesis, Ohio State University, (1979).

Scan No. 1

DEGREES

TYPE SCAN	-30	-27.5	-25	-22.5	-20	-17.5	-15	-12.5	-10	-7.5	-5	-2.5	0	2.5	5	7.5	10	12.5	15	17.5	20	22.5	25	27.5	30
AIR	2869	2063	2084	2315	2404	2447	2485	2490	2516	2528	2534	2532	2527	2522	2526	2513	2492	2471	2449	2398	2308	2149	1743	2834	2842
46% VOID	2875	2109	1573	1518	1483	1448	1435	1434	1443	1456	1465	1464	1470	1469	1463	1466	1456	1423	1452	1464	1482	1541	1703	2830	2832
40% VOID	2826	2100	1552	1469	1402	1380	1351	1339	1332	1345	1349	1348	1342	1348	1361	1345	1357	1342	1364	1384	1422	1497	1667	2835	2846
30% VOID	2857	2061	1517	1377	1278	1218	1176	1160	1146	1130	1133	1126	1136	1139	1141	1158	1171	1176	1209	1269	1314	1430	1646	2835	2837
20% VOID	2864	2074	1500	1331	1218	1133	1079	1055	1018	1010	1002	1001	999	1005	1018	1023	1048	1077	1125	1198	1261	1390	1630	2824	2819
10% VOID	2879	2035	1505	1308	1173	1082	1005	958	913	894	884	876	894	894	902	923	952	991	1041	1127	1218	1370	1632	2800	2815
WATER	2885	2062	1495	1266	1106	996	913	858	811	781	758	748	740	745	765	790	826	877	951	1044	1153	1359	1663	2850	2835
WALNUT (ρ=.732)	2853	2082	1742	1565	1449	1392	1335	1265	1206	1159	1141	1121	1126	1108	1113	1132	1161	1207	1282	1365	1458	1619	1705	2816	2846
PINE (ρ=.41)	2858	2060	1773	1863	1800	1754	1705	1678	1639	1616	1601	1599	1595	1594	1610	1621	1645	1669	1715	1750	1782	1856	1710	2834	2827

Scan No. 2

DEGREES

TYPE SCAN	-30	-27.5	-25	-22.5	-20	-17.5	-15	-12.5	-10	-7.5	-5	-2.5	0	2.5	5	7.5	10	12.5	15	17.5	20	22.5	25	27.5	30
AIR													2574												2878
40% VOID	2901	2124	1563	1485	1429	1378	1359	1356	1358	1350	1374	1380	1387	1392	1389	1379	1386	1380	1387	1403	1435	1525	1749	2873	2883
30% VOID	2914	2103	1548	1411	1322	1268	1218	1203	1186	1183	1184	1181	1188	1193	1196	1203	1225	1246	1272	1322	1359	1476	1737	2862	2879
20% VOID	2907	2089	1541	1379	1266	1188	1126	1097	1062	1018	1043	1038	1040	1048	1047	1077	1090	1123	1176	1236	1310	1453	1735	2682	2874
10% VOID	2902	2090	1532	1342	1198	1108	1037	985	950	922	907	908	910	919	932	959	975	1020	1093	1166	1254	1435	1724	2883	2885
WATER													746												

Scan No. 3

DEGREES

TYPE SCAN	-30	-27.5	-25	-22.5	-20	-17.5	-15	-12.5	-10	-7.5	-5	-2.5	0	2.5	5	7.5	10	12.5	15	17.5	20	22.5	25	27.5	30
AIR													2605												2917
40% VOID	2944	2156	1595	1509	1440	1404	1349	1370	1386	1381	1399	1401	1426	1411	1424	1421	1400	1411	1432	1442	1472	1550	1767	2936	2938
30% VOID	2965	2172	1589	1447	1379	1308	1283	1257	1247	1236	1254	1256	1251	1249	1263	1276	1277	1285	1308	1358	1386	1504	1750	2910	2912
20% VOID	2949	2119	1550	1380	1253	1185	1136	1097	1072	1054	1050	1063	1077	1073	1079	1088	1128	1152	1188	1241	1330	1480	1759	2920	2917
10% VOID	2950	2120	1542	1342	1203	1110	1038	991	948	942	926	918	922	924	955	973	990	1043	1096	1170	1279	1454	1743	2917	2926
WATER													763												

Scan No. 4

DEGREES

TYPE SCAN	-30	-27.5	-25	-22.5	-20	-17.5	-15	-12.5	-10	-7.5	-5	-2.5	0	2.5	5	7.5	10	12.5	15	17.5	20	22.5	25	27.5	30
AIR													2575												2893
40% VOID	2895	2124	1574	1501	1443	1426	1405	1396	1406	1424	1413	1421	1422	1438	1414	1422	1413	1418	1410	1416	1446	1524	1728	2868	2860
30% VOID	2890	2095	1543	1416	1312	1278	1224	1206	1203	1195	1197	1200	1210	1208	1221	1209	1239	1248	1264	1307	1372	1486	1735	2857	2860
20% VOID	2884	2080	1530	1351	1234	1170	1105	1061	1041	1040	1026	1030	1034	1038	1049	1053	1087	1122	1171	1225	1303	1456	1722	2856	2853
10% VOID	2885	2075	1518	1311	1181	1083	1007	964	926	905	891	889	882	895	906	927	962	1014	1070	1151	1246	1421	1726	2860	2862
WATER													759												

Scan No. 5

DEGREES

TYPE SCAN	-30	-27.5	-25	-22.5	-20	-17.5	-15	-12.5	-10	-7.5	-5	-2.5	0	2.5	5	7.5	10	12.5	15	17.5	20	22.5	25	27.5	30
AIR													2565											2870	
40% VOID	2903	2130	1572	1501	1443	1408	1373	1374	1380	1381	1390	1391	1416	1409	1407	1413	1403	1402	1411	1438	1466	1548	1746	2886	2901
30% VOID	2900	2117	1570	1462	1361	1311	1256	1248	1226	1233	1235	1240	1244	1233	1239	1246	1264	1280	1298	1349	1395	1517	1747	2890	2891
20% VOID	2910	2116	1563	1455	1344	1269	1224	1187	1161	1145	1136	1137	1144	1137	1140	1155	1180	1198	1224	1280	1358	1501	1733	2869	2866
12% VOID	2903	2134	1573	1439	1323	1223	1173	1117	1088	1052	1036	1029	1035	1032	1048	1072	1106	1132	1197	1267	1364	1520	1732	2879	2872
WATER													750												

Scan No. 6

DEGREES

PE SCAN	-30	-27.5	-25	-22.5	-20	-17.5	-15	-12.5	-10	-7.5	-5	-2.5	0	2.5	5	7.5	10	12.5	15	17.5	20	22.5	25	27.5	30
AIR													2575												2900
VOID	2897	2123	1566	1499	1428	1391	1355	1352	1340	1342	1361	1364	1367	1369	1379	1372	1370	1369	1402	1411	1460	1531	1739	2895	2885
VOID	2916	2121	1559	1413	1316	1237	1194	1174	1164	1145	1141	1143	1144	1153	1154	1169	1174	1218	1234	1290	1352	1474	1729	2866	2875
VOID	2909	2091	1534	1356	1227	1159	1090	1052	1026	1010	997	1001	1006	999	1027	1035	1065	1108	1159	1212	1287	1452	1729	2874	2882
VOID	2906	2102	1521	1308	1172	1079	1009	967	918	907	881	887	886	894	908	930	972	1011	1080	1146	1258	1423	1729	2884	2879
WATER													757												

A P P E N D I X B

```
C ***********************************************************************
C       PROGRAM TO COMPUTE LINE INTEGRAL OF A GIVEN FUNCTION OF
C       TWO VARIABLES
C       DEFINITIONS :
C             A=LOWER LIMIT
C             B=UPPER LIMIT
C             D=NUMBER OF DIVISIONS
C             M=SLOPE OF THE GIVEN LINE
C             C=Y INTERCEPT
C             N=NUMBER OF READINGS FOR EACH VALUE OF THE SLOPE M
C ***********************************************************************

      REAL M
      OPEN(UNIT=1,FILE='SUP3.DAT')
      READ(1,*)A,B,D,M,C

      OPEN(UNIT=2,FILE='SUP30.DAT')
      WRITE(5,10)
      WRITE(2,10)
10    FORMAT(19X,'THETA',15X,'S',13X,'PROJ.DATA'///)

      PI=4.*ATAN(1.)
      C=C-.1
      H=(B-A)/D
      T=ATAN(M)
      T=T-PI/18.

C .....Compute for different values of M.
      DO 500 I=1,18

25        T=T+PI/18.
          R=T*180./PI
          XA=ABS(R-89.99)

C     BRANCH FOR THE CONDITION WHEN RAYS ARE PARALLEL TO THE Y-AXIS

          IF(XA.LT.1.)CALL SUB1(R,T,A,B,D,M,C)

          C=-1.1/COS(T)
          M=TAN(T)
          S=-1.1

        DO 500 N=1,21
          S=S+0.1
C
C.....THE 'IF-THEN-ELSE'STRUCTURE HELPS IN OVERCOMING THE ERROR

C.....IN THE TWENTY-FIRST ITERATION.
C
```

```
                IF(N.LE.20)THEN
                C=C+0.1/COS(T)
                ELSE
                C=C+.10001/COS(T)
                ENDIF
                A=B-D*H
                S1=F(A,M,C)+F(B,M,C)
C
C .......Compute the number of times the do loop is to be executed.
C
                K=NINT(D/2.-1.)
C
C         COMPUTE THE SUM OF ODD TERMS
C
                SO=0.
                A=A+H
                DO 100 KI=1,K
                  P=F(A,M,C)
                  SO=SO+P
                  A=A+2.*H
100             CONTINUE

C         INITIALIZE A FOR COMPUTING THE SUM OF EVEN TERMS

                  A=B-(D-2.)*H

C
C         COMPUTE THE SUM OF EVEN TERMS
C
                  SE=0.
                 DO 200 KJ=1,K
                    Q=F(A,M,C)
                    SE=SE+Q
                    A=A+2.*H
200              CONTINUE
C
C         APPLY SIMPSON'S ONE-THIRD RULE
C
                   DI=(H/3.)*(S1+(4.*SO)+(2.*SE))*(SQRT(1.+M**2))
                   R=T*180./PI
                   WRITE(5,400)R,S,DI
                   WRITE(2,400)R,S,DI
500       CONTINUE
          STOP
400       FORMAT(13X,F15.8,3X,F12.2,7X,F13.8)
C
C .......End of main program.
C
          END
C
C ***************************************************************************
C
```

```
C       THIS FUNCTION DEFINES THE VALUE OF F(X,Y) ALONG ALL LINES
C       OTHER THAN THE Y-AXIS AND LINES PARALLEL TO IT.
C
C*************************************************************************
C
        FUNCTION F(X,M,C)
        REAL M
        Y=M*X+C
        SQ=Y**2+X**2
        IF(SQ.LT.1.)THEN
        F=1.
        ELSE
        F=0.
        ENDIF
        RETURN
        END
C
C ************************************************************************
C
C       THIS FUNCTION DEFINES THE VALUE OF F(X,Y) ALONG THE Y-AXIS
C       AND LINES PARALLEL TO IT.
C
C ************************************************************************
C
        FUNCTION G(M,C,Y)
        REAL M
        SQ1=Y**2+C**2
        IF(SQ1.GE.1.)THEN
        G=0.
        ELSE
        G=1.
        ENDIF
        RETURN
        END
C  ************************************************************************
        SUBROUTINE SUB1(R,T,A,B,D,M,C)
        REAL M
C
        PI=4.*ATAN(1.)
C
C       THE FUNCTION DEFINITION ENSURES THAT ,IF DESIRED,INTEGRALS OUTSIDE A
C       UNIT CIRCLE ARE ZERO.
C
C       WE HAVE TO RESORT TO A SUBROUTINE , BECAUSE FOR THE Y-AXIS,
C       THE SLOPE 'M' IS INFINITY. THE ESSENTIAL DIFFERENCE BETWEEN
C       THE SUBROUTINE AND THE MAIN PROGRAM IS THAT, FOR COMPUTING
C       THE LINE INTEGRAL, ONLY THE LIMITS ON Y NEED TO BE KNOWN

            A=-1.0
            B=1.0
            H=(B-A)/D
            C=-1.1
```

```
            DO 501 N=1,21
              IF(N.LE.20)THEN
              C=C+.1
              ELSE
              C=C+.10001
              ENDIF
              A=B-D*H
              S1=G(M,C,A)+G(M,C,B)
C
C .......Compute the number of times the do loop is to be execute
C
              K=NINT(D/2.-1.)
C
C         COMPUTE THE SUM OF ODD TERMS
C
              SO=0.
              A=A+H
              DO 101 KI=1,K
                   P=G(M,C,A)
                   SO=SO+P
                   A=A+2.*H
101           CONTINUE
              A=B-(D-2.)*H
C
C         COMPUTE THE SUM OF EVEN TERMS
C
              SE=0.
              DO 201 KJ=1,K
                   Q=G(M,C,A)
                   SE=SE+Q
                   A=A+2.*H
201           CONTINUE
C
C         APPLY SIMPSON'S ONE-THIRD RULE
C
              DI=(H/3.)*(S1+(4.*SO)+(2.*SE))
              R=90.
              WRITE(5,400)R,C,DI
              WRITE(2,400)R,C,DI
501       CONTINUE
C
C         UPDATE THE VALUE OF THE ANGLE TO R=100. DEGREES.
C
          T=T+PI/18.
400       FORMAT(13X,F15.8,3X,F12.2,7X,F13.8)
          RETURN
          END
```

A P P E N D I X C

```
C**********************************************************************
C       PROGRAM FOR FAN-BEAM DATA.
C**********************************************************************

C**********************************************************************
C       P(41)=MATRIX OF THE PROJECTED DATA
C       FAN(756,3)=MATRIX OF FAN-BEAM DATA CONVERTED TO PARALLEL
C       Q(41)=MATRIX OF FILTER VALUES
C       Q1(41,41)=MATRIX OF 'Q' VALUES PROJECTED DIAGONALLY
C       PIC1(41)=MATRIX OF CONVOLVED VALUES
C       PIC(41,41)=MATRIX OF  VALUES FROM PREVIOUS SCAN
C       FPIC(41,41)=FINAL PICTURE
C       IPIC(41,41)=INTEGER VALUES OF FPIC FOR SCREEN DISPLAY
C**********************************************************************

        DIMENSION FAN(756,3),P(41),Q(41),Q1(41,41),PIC(41,41),PIC1(
        DIMENSION IPIC(41,41),FPIC(41,41),TEMP(3),PROJ(378,2),DEN(2

C**********************************************************************
C       RAM.FIL CONTAINS THE 'Q' VALUES
C       PIC.DAT STORES THE VIEW AT A GIVEN ANGLE
C       FPIC.DAT STORES THE IMAGE AFTER EVERY ITERATION
C       DIV.DAT CONTAINS THE NUMBER OF PIXELS IN A ROW
C       P1D.T10 CONTAINS PROJECTED DATA
C       AIR.REF CONTAINS THE DATA FOR PLEXIGLASS CORRECTION
C**********************************************************************

        OPEN(UNIT=20,FILE='RAM.FIL')
        OPEN(UNIT=22,FILE='DIV1D.T10')
        OPEN(UNIT=26,FILE='P1D.T10')
        OPEN(UNIT=23,FILE='DIV.DAT')
        OPEN(UNIT=28,FILE='AIR.REF')

          PI=4.*ATAN(1.)

C       READ INPUT PARAMETERS

          READ(23,*)NDIV,NVIEW,D,RAD
          SGMAX=D*SIN(25.*PI/180.)

        DO 75 I=1,378
           READ(26,*)BETA,SGMA,DATA
           FAN(I,1)=BETA+SGMA
           FAN(I,2)=D*SIN(SGMA*PI/180.)/SGMAX
           FAN(I,3)=DATA
75      CONTINUE
```

```
C       INTERPOLATION
              I=1
        DO 80 J=1,18
              XX=-1.0
              PROJ(I,1)=XX
              PROJ(I,2)=FAN(1,3)
           DO 80 K=1,21
              I=I+1
              IF(I.GT.378)GOTO 65
              XX=XX+.1
              XX1=FAN(I-1,2)
              XX2=FAN(I,2)
              YY1=FAN(I-1,3)
              YY2=FAN(I,3)
              PROJ(I,1)=XX
              PROJ(I,2)=YY1-((XX1-XX)*(YY1-YY2)/(XX1-XX2))
80      CONTINUE
C       READ THE DATA FOR PLEXIGLASS CORRECTION INTO AN ARRAY
65      READ(28,51)((DEN(M,N),M=1,21),N=1,21)

C
C       INITIALIZE ALL PIXELS TO ZERO
C
        DO 500 I=1,NDIV
           DO 500 J=1,NDIV
             FPIC(I,J)=0.
             PIC(I,J)=0.
             IPIC(I,J)=0
500     CONTINUE

C       READ IN THE VALUES OF THE Q FUNCTION, FOR CONVOLUTION
        READ(20,11)(Q(N),N=1,NDIV)

C       DISPLAY FORMAT MESSAGE

        WRITE(5,10)
        WRITE(22,10)
C
C       SPREAD ELEMENTS OF Q ALONG DIAGONALS OF Q1
C
           DO 101 N1=1,NDIV
           DO 101 M1=1,NDIV
              NMD=ABS(N1-M1)+1
              Q1(N1,M1)=Q(NMD)
101        CONTINUE

C
C       START VIEWING AT DIFFERENT ANGLES
C
        X=0.
        KK=0
```

```
      DO 700 I=0,(NVIEW-1)
      X=X+1.

      I3=0
      DO 81 II=1,NDIV
            I3=I3+1
            KK=KK+1
            P(II)=-LOG(PROJ(I3,2))
81    CONTINUE

C
C     CARRY OUT CONVOLUTION
C
          DO 200 II=1,NDIV
             PIC1(II)=0.
               DO 200 J1=1,NDIV
                  PIC1(II)=PIC1(II)+(Q1(II,J1)*P(J1))
200       CONTINUE

         T=REAL(I)*PI/REAL(NVIEW)

C
C     ADJUST FOR OVERLAP FOR DIFFERENT VIEWS
C

         NDV=NDIV/2+1
         NDV1=NDV-1

         DO 699 M1=-NDV1,NDV1
            DO 699 N1=-NDV1,NDV1
              M=M1+NDV
              N=N1+NDV
              RM=REAL(M)
              RN=REAL(N)
              DSQ=ABS(SQRT((RM-NDV)**2+(RN-NDV)**2))

                IF(RM.EQ.NDV)THEN
                 PHI=PI/2.
                 ELSE
                PHI=ATAN((RN-NDV)/(RM-NDV))
                 ENDIF

              R=(DSQ*COS(T-PHI))+NDV
              L=INT(R)
      IF(L.LT.1.OR.L.GT.20)GOTO 699

          S=(R-REAL(L))*(PIC1(L+1)-PIC1(L))+PIC1(L)
          Z=(2.0*PI*(REAL(NVIEW))*REAL(NDIV-1))/(REAL(NDIV**2)
      PIC(M,N)=FPIC(M,N)
      FPIC(M,N)=((FPIC(M,N)*(X-1.))+((S*Z-DEN(M,N))/RAD))/X

C     EQUATE THE PIXEL VALUES OUTSIDE CIRCLE TO ZERO
```

```
            MSQ=(M-NDV)**2+(N-NDV)**2
               IF(MSQ.GT.NDV1**2)THEN
                 FPIC(M,N)=0.00
               ELSE
               ENDIF

      IPIC(M,N)=ABS(NINT(FPIC(M,N)*100.))

699   CONTINUE

C     THIS OPTION ALLOWS US TO TERMINATE THE PROCEEDINGS IF THE ERROR OF
C     RECONSTRUCTION REACHES A PRESET LOWER LIMIT

      SDIS=0.
      SPIC=0.
      DO 695 M=1,NDIV,3
         DO 695 N=1,NDIV,3
            DIS=ABS((FPIC(M,N)-PIC(M,N)))
            SDIS=SDIS+DIS
            SPIC=SPIC+ABS(FPIC(M,N))
695   CONTINUE
      IF(SDIS.LT.(.005*SPIC))GOTO 694

               DEG=180.*T/PI
               WRITE(5,50)((IPIC(M,N),N=1,NDIV),M=1,NDIV)
               WRITE(5,111)DEG
               WRITE(21,111)DEG

50    FORMAT(21(6X,21(I3)/)/)
51    FORMAT(21(8X,F14.8/)/)
15    FORMAT(8X,A72///)
100   FORMAT(50X,F13.8)
111   FORMAT(45X,F10.5,2X,'DEGREES')
700   CONTINUE

694                WRITE(22,50)((IPIC(M,N),N=1,NDIV),M=1,NDIV)

C     CALCULATE THE MAXIMUM AND MINIMUM PIXEL (LITE) VALUES

      RMIN=0.
      RMAX=0.

      DO 800 I=1,NDIV
         DO 800 J=1,NDIV
            IF(FPIC(I,J).GT.RMAX)RMAX=FPIC(I,J)
            IF(FPIC(I,J).LT.RMIN)RMIN=FPIC(I,J)
800   CONTINUE
      WRITE(22,13)RMAX,RMIN

C     CALCULATE THE AVERAGE PIXEL (LITE) VALUE

      SUM=0.
```

```
      DTR=0.
      DO 900 I=5,NDIV-4
         DO 900 J=5,NDIV-4
            SUM=SUM+FPIC(I,J)
            DTR=DTR+1.
900   CONTINUE
      AVG=SUM/DTR

      WRITE(22,12)NDIV,NDV
      WRITE(22,51)(FPIC(11,N),N=1,NDIV)
      WRITE(22,14)AVG
      WRITE(5,*)AVG,DTR
      WRITE(22,51)((FPIC(M,N),M=1,NDIV),N=1,NDIV)
12    FORMAT(2X,'HORIZONTAL CENTERLINE'/,'ROW',I2/,'COLUMN 1 TO',.
13    FORMAT(2X,'MAXIMUM LITF=',2X,F14.8,2X,'MINIMUM LITF=',F14.8
14    FORMAT(2X,'AVERAGE=',F14.8//)
      STOP
10    FORMAT(2X,'POSITIVE IMAGE'//,2X,'FPIC.DAT'//,2X,'RAM.FIL')
11    FORMAT(3(9X,E15.7))
      END
```

A P P E N D I X D

```
{TO GENERATE A SERIES OF RANDOM NUMBERS AND SUPERIMPOSE  THEM  ON
DATA.}
PROGRAM MCV;
VAR
   R,SQRT1:REAL;
   C,N,SQRT2,NPOT:INTEGER;
   IP,OP:TEXT;
BEGIN
ASSIGN(IP,'C:T10DD.DAT');
RESET(IP);
ASSIGN(OP,'C:POL1D.T10');
REWRITE(OP);
       C:=1;
       WHILE C <=21 DO
        BEGIN
         READLN(IP,R,N);
         SQRT1:=SQRT(N);
         SQRT2:=ROUND(SQRT1);
         NPOI:=2*RANDOM(SQRT2)-SQRT2;
         N:=N+(1*NPOI);
         WRITELN(OP,R:10:3,N:10);
         C:=C+1;
        END;  {WHILE}
        CLOSE(OP);
END.  {RANDNUM}
```

A P P E N D I X E

RECONSTRUCTED IMAGE FOR PINE.

POSITIVE IMAGE

FPIC.DAT

RAM.FIL

0	0	0	0	0	0	0	0	0	0	5	0	0	0	0	0	0	0	0	0	0
0	0	0	0	0	0	5	6	7	7	7	7	7	7	7	0	0	0	0	0	0
0	0	0	0	4	6	7	8	8	8	8	8	8	8	8	7	7	7	0	0	0
0	0	0	5	7	8	8	8	8	8	8	8	8	8	8	7	7	7	0	0	0
0	0	4	7	8	8	8	8	8	8	8	8	8	8	8	8	7	7	7	0	0
0	0	6	8	8	8	8	8	8	8	8	8	8	8	8	8	8	7	7	0	0
0	5	7	8	8	8	8	8	8	9	9	9	9	8	8	8	8	8	7	7	0
0	6	8	8	8	8	8	8	9	9	9	9	9	9	8	8	8	8	7	7	0
0	7	8	8	8	8	8	9	9	9	9	9	9	9	9	8	8	8	8	7	0
0	7	8	8	8	8	8	9	9	9	9	9	9	9	9	8	8	8	8	7	0
5	7	8	8	8	8	8	9	9	9	9	9	9	9	8	8	8	8	8	7	5
0	7	8	8	8	8	9	9	9	9	9	9	9	9	8	8	8	8	8	7	0
0	7	8	8	8	8	9	9	9	9	9	9	9	9	8	8	8	8	8	7	0
0	7	7	8	8	8	8	9	9	9	9	9	9	8	8	8	8	8	8	6	0
0	7	7	8	8	8	8	8	9	9	9	9	8	8	8	8	8	8	7	5	0
0	0	7	7	8	8	8	8	8	8	8	8	8	8	8	8	8	8	6	0	0
0	0	7	7	7	8	8	8	8	8	8	8	8	8	8	8	8	7	4	0	0
0	0	0	7	7	7	8	8	8	8	8	8	8	8	8	8	7	5	0	0	0
0	0	0	0	7	7	7	8	8	8	8	8	8	8	7	6	4	0	0	0	0
0	0	0	0	0	0	7	7	7	7	7	7	7	6	5	0	0	0	0	0	0
0	0	0	0	0	0	0	0	0	0	5	0	0	0	0	0	0	0	0	0	0

MAXIMUM LITF= 0.08874133 MINIMUM LITF= -0.05289834

HORIZONTAL CENTERLINE

ROW21

COLUMN 1 TO 11

0.05009277
0.07049052
0.07905515
0.07876664
0.08131342
0.08379398
0.08468780
0.08708410
0.08687436
0.08755311
0.08603749
0.08753311

0.08687436
0.08708610
0.08468780
0.08379398
0.08131342
0.07876664
0.07905515
0.07049052
0.05009277

AVERAGE= 0.08329582

0.00000000
0.00000000
0.00000000
0.00000000
0.00000000
0.00000000
0.00000000
0.00000000
0.00000000
0.00000000
0.05009277
0.00000000
0.00000000
0.00000000
0.00000000
0.00000000
0.00000000
0.00000000
0.00000000
0.00000000
0.00000000

0.00000000
0.00000000
0.00000000
0.00000000
0.00000000
0.00000000
0.04868446
0.05963553
0.06622172
0.06966973
0.07049052
0.06845242
0.06726465
0.06780012
0.06966886
0.00000000

0.00000000
0.00000000
0.00000000
0.00000000
0.00000000

0.00000000
0.00000000
0.00000000
0.00000000
0.04300825
0.06167946
0.07129160
0.07613724
0.07821389
0.07920318
0.07905515
0.07844675
0.07728843
0.07486982
0.06928518
0.06817999
0.07150093
0.00000000
0.00000000
0.00000000
0.00000000

0.00000000
0.00000000
0.00000000
0.04754804
0.06619010
0.07559633
0.07900287
0.07886074
0.07843288
0.07870436
0.07876664
0.07904380
0.07807133
0.07781857
0.07748792
0.07406854
0.06755796
0.07019676
0.00000000
0.00000000
0.00000000